Journal of Control, Automation and Electrical Systems (2020) 31:1177–1195
https://doi.org/10.1007/s40313-020-00599-4

Chattering-Free Trajectory Tracking Robust Predefined-Time Sliding Mode Control for a Remotely Operated Vehicle

Pooyan Alinaghi Hosseinabadi[1] · Ali Soltani Sharif Abadi[2] · Saad Mekhilef[1,3,4] · Hemanshu Roy Pota[5]

Received: 8 February 2020 / Revised: 15 April 2020 / Accepted: 16 April 2020 / Published online: 14 May 2020

Abstract

This study investigates a new chattering-free robust predefined-time sliding mode control (CFRPSMC) scheme for the trajectory tracking control problem of a three-degree-of-freedom (3-DOF) remotely operated vehicle (ROV) in the presence of matched uncertainties. The advanced notion of predefined-time stability is used to provide a maximum convergence time as desired that can be set during the control design and independently of the initial conditions. Based on defining a new form of sliding surfaces, a new control law is designed to ease the undesirable chattering phenomenon without damaging the robustness properties and tracking precision. The proposed control scheme can not only solve the predefined-time tracking controller design problem, but also provide the robustness to various uncertainties. The Lyapunov stability theory is used to establish the stability analysis of the closed-loop system in both the reaching phase and the sliding phase. The performance of the proposed CFRPSMC scheme is evaluated for the 3-DOF ROV through two comparative simulation cases using Simulink/MATLAB. The comparative simulation results and analytical comparisons demonstrate the efficacy and superiority of the proposed method compared with other relevant conventional methods.

Keywords Predefined time · Sliding mode · Robust · ROV · Tracking · Chattering-free

1 Introduction

It is now possible to use an ROV for underwater exploration for a risky mission (Hosseinabadi 2018). The ROV has attracted interest due to its important role in the underwater exploration including military applications, oceanographic mapping, inspection of the pipeline, pipeline maintenance, mineral exploration, and oil and gas exploration. Lack of accurate ROV kinematic model might lead to the extremely ROV nonlinear dynamics, which is called parametric uncertainty. Because of the change in water density, the weight of the ROV is likely to change, namely, the modelling uncertainty. Hence, ROV research is challenging because of the modelling uncertainty and parametric uncertainty (Wang et al. 2016a; Hosseinabadi 2018). It should be noted that the sum of these modelling uncertainty and parametric uncertainty is called uncertainties throughout the paper.

To fully utilize the potential of the ROVs in underwater tasks, trajectory tracking problem with good precision and fast convergence has attracted the interest of many researchers (Da Cunha et al. 1995; Zhu and Gu 2011; Wei et al. 2015; Fernandes et al. 2013; Abadi and Hosseinabadi 2017). Two basic shortcomings of the incipient approaches

✉ Pooyan Alinaghi Hosseinabadi
pooyanalinaghi@um.edu.my

Ali Soltani Sharif Abadi
a.soltanisharif@stu.yazd.ac.ir

Saad Mekhilef
saad@um.edu.my; smekhilef@swin.edu.au

Hemanshu Roy Pota
h.pota@adfa.edu.au

1 Power Electronics and Renewable Energy Research Laboratory (PEARL), Department of Electrical Engineering, Faculty of Engineering, University of Malaya, Kuala Lumpur 50603, Malaysia

2 Department of Electrical Engineering, Faculty of Engineering, Yazd University, Yazd, Iran

3 School of Software and Electrical Engineering, Swinburne, Melbourne, VIC, Australia

4 Center of Research Excellence in Renewable Energy and Power Systems, King Abdulaziz University, Jeddah 21589, Saudi Arabia

5 School of Engineering and Information Technology, The University of New South Wales, Canberra, ACT, Australia

to overcome the trajectory tracking issue are classified as follows: Firstly, they are not robust against uncertainties of ROVs (Da Cunha et al. 1995; Fernandes et al. 2013). Secondly, they are only able to achieve the globally asymptotic stability with infinite settling time (Da Cunha et al. 1995; Fernandes et al. 2013; Wei et al. 2015; Zhu and Gu 2011). However, the VS-MRAC scheme proposed in Da Cunha et al. (1995) has been reported as a robust algorithm with respect to substantial unmodelled dynamics and even delays. The issue concentrating on heading motion control for ROV has been investigated, and an adaptive integral back-stepping control scheme with nonlinear disturbance observer was suggested in Wei et al. (2015). Integral terms have been added into the feedback loop to develop the system's robust performance. The results in Wei et al. (2015) show that the controller would tackle and approximate factors including the uncertainty model. The system can track the reference trajectory precisely and with a high robustness to parametric uncertainty. In Ettefagh et al. (2017), a novel Lyapunov function has been defined to ensure asymptotic stability of the linear time-varying system. In (Berdnikov and Lokhin 2019), the system asymptotic stability has been ensured using new spline Lyapunov functions instead of classical quadratic Lyapunov functions which provide bigger stability regions. However, the above-mentioned studies have not dealt with the notions of finite-/fixed-/predefined-time stability which are often necessary to consider in many practical applications.

To overcome the first deficiency, SMC method has been used to deal with uncertainties of ROVs (Pezeshki et al. 2016; Dyda et al. 2016; Chin and Lin 2018; Khalid et al. 2019). SMC has been known as an effective control method for nonlinear uncertain systems because of its fast response, robustness against uncertainties, unresponsiveness to external disturbances and its easy implementation (Mobayen et al. 2017). The basic idea of SMC is to force the system state trajectories (by applying a designed control law to the system) to slide onto the sliding surface (specific switching manifold) and to define a sliding surface such that tracking errors reach zero along with the sliding surface. SMC scheme has also been employed for different applications to ensure the robustness feature of the controllers (Tchinda et al. 2019; Taheri et al. 2019; Van Nguyen et al. 2019; Zaihidee et al. 2019; Eaton et al. 2009; Shafiei and Binazadeh 2013; Yousefi and Binazadeh 2018; Elsayed et al. 2015). On the other hand, SMC individually merely guarantees asymptotic stability of the system to which it is applied. To cater for this drawback and to enable the system to have a finite-time state convergence, terminal SMC (TSMC), TSMC has been designed for various systems (Mobayen 2015; Abadi et al. 2018a, b; Song et al. 2018; He et al. 2017; Tiwari et al. 2015; Hosseinabadi and Abadi 2019; Boonsatit and Pukdeboon 2016; Homaeinezhad et al. 2020). The TSMC possesses the advantage of the SMC, improves system stability and performance, and accelerates the convergence time around the equilibrium point (Zhou et al. 2015). These features have led to the design of TSMC for ROVs (Wang et al. 2014, 2015, 2016b, 2018).

On the other hand, the presented finite settling time (using finite-time control methods) is not independent of the initial conditions that would limit its practical applications because of likely unknown initial conditions of the system. To surmount the above, Polyakov has introduced the fixed-time stability method in 2012 (Polyakov 2011). This method gives a bounded convergence time independent of initial conditions. The notion of fixed-time stability has been studied in (Parsegov et al. 2012, 2013; 2015). A novel combination of a nonsingular SMC scheme and fixed-time stability method has been presented for second-order systems (Zuo 2014). However, the chattering problem is observed in the control signal of this study. Although the notion of fixed-time stability is superior to the finite-time stability notion, there is no direct relationship between the convergence time-bound and the system parameters, which is necessary for many control problems that need to satisfy hard time constraints (Sánchez-Torres et al. 2018b). To cope with this shortage, the notion of predefined-time stability has been presented in Sánchez-Torres et al. (2015, 2018a) and Jiménez-Rodríguez et al. (2017a). Using the predefined-time stability notion in the controller provides a class of fixed-time controller with convergence time-bound as an explicit parameter which can be determined as desired in advance. Worded in another way, in the predefined-time methods, the fixed convergence time-bound is a tunable parameter. This advanced stability notion has been incorporated with the SMC method to control different systems. It can be pointed out in the work of Becerra et al. (2017) that a high-order integral system has been controlled using a predefined-time SMC (PSMC) scheme. A robust controller has been designed in Munoz-Vazquez et al. (2019) using PSMC scheme for manipulators. In Sánchez-Torres et al. (2018a), a new PSMC scheme has been presented for a class of second-order systems. However, the chattering problem exists in this method due to using signum function in the control law and no effort has been made to alleviate it.

The SMC scheme often causes the unwanted chattering phenomenon due to its discontinuous nature of the control law in the existing studies using SMC method (Eaton et al. 2009; Yousefi and Binazadeh 2018; Shafiei and Binazadeh 2013; Dyda et al. 2016), TSMC method (Feng et al. 2002; Yu and Zhihong 2002; Mobayen 2015), fixed-time SMC (FSMC) method (Zuo 2014) and PSMC method (Sánchez-Torres et al. 2018a). The inherent chattering of conventional SMC needs ample energy for high efficiency, and it might damage the system's physical parts (Castillo-García et al. 2017). Many studies in the literature have made efforts to alleviate or eliminate this problem. In (Badfar et al. 2020), the chattering phenomenon in the con-

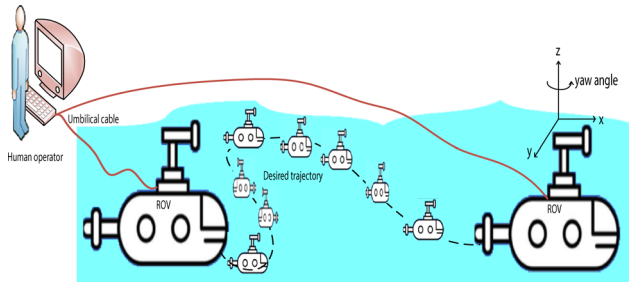

Fig. 1 Structure of trajectory tracking for the 3-DOF ROV

trol input signal of the proposed finite-time SMC method has been eliminated by replacing the hyperbolic tangent function instead of the signum function. However, the stability analysis of the closed-loop system using a hyperbolic tangent function in control law has not been established in this study. In Benosman and Lum (2009) and Yang and Yang (2011), approximating signum function in controllers by saturation or sigmoid functions managed to reduce this problem. However, these approaches created large steady-state errors, due to the boundary layer around sliding surfaces. Motivated by above discussion, in this paper, we aim to investigate the problem of designing a new chattering-free robust predefined-time controller on the basis of SMC theory for trajectory tracking of a 3-DOF ROV in the presence of uncertainties, which is yet to be developed based on our knowledge.

Therefore, focusing on the major issues for ROV control including trajectory tracking problem, the presence of uncertainties, unavailability of initial conditions (for determining the system convergence time in advance), fulfilling hard time constraints, chattering problem and stability, a new CFRPSMC method is proposed. This proposed method is aimed to design a robust tracking controller against uncertainties of a nonlinear 3-DOF ROV on the basis of SMC theory with predefined-time convergence. This trajectory tracking controller is used to control a ROV with 3 DOFs which are the position (x, y) and the orientation (yaw angle) of ROV in planes parallel to the sea surface. ROV is aimed to track a desired plane (desired trajectory) with 3 DOFs (x, y and yaw angle) by using the proposed trajectory tracking controller. The structure of trajectory tracking control for the 3-DOF ROV is illustrated in Fig. 1. Note that ROV has an umbilical cable for communication, controlling the vehicle depth and providing power by a human operator.

The undesirable chattering phenomenon (which is a common problem with the conventional SMC) is eliminated by defining new forms of sliding surfaces and control laws. Lyapunov stability theory is utilized to establish predefined-time stability analysis of closed-loop system based on SMC technique. An accurate comparison is made between the proposed CFRPSMC scheme and an RPSMC scheme with conventional forms of sliding surfaces and control laws to demonstrate the effectiveness of the proposed sliding surfaces and control laws in eliminating the chattering problem. The effectiveness of the notion of predefined-time stability in the proposed CFRPSMC method is demonstrated by comparing this method with the other two methods with no predefined time: FSMC and TSMC. It should be noted that the ideas behind designing FSMC and TSMC schemes (which are presented and simulated in this paper) are similar to the ones given in Zuo (2014) and Zuo and Tie (2016), respectively. Additionally, the proposed CFRPSMC scheme is compared with a relevant study for the 3-DOF ROV given in Dyda et al. (2016) to verify the validity of the proposed scheme. For a thorough comparison, three well-known performance criteria are used.

Compared with the existing works, the main contributions of this paper can be highlighted as follows:

(1) In this paper, the matched uncertainties are considered in controlled systems, by considering bounded uncertainties in CFRPSMC design. Hence, the proposed control method can solve the predefined-time tracking controller design problem in the presence of uncertainties, in addition to having robustness to uncertainties.
(2) Based on defining a new form of sliding surfaces, a new control law is designed (where the integral of signum function is used) to eliminate the chattering phenomenon and fulfil trajectory tracking in a predefined time.
(3) The proposed CFRPSMC method presents a desired maximum convergence time which is a tunable parameter. That is, the upper bound of convergence time can be set during the control design and independently of initial conditions.
(4) The proposed control method is applicable for predefined-time stabilizing and trajectory tracking of an extensive class of nonlinear double integrator systems.
(5) Some design parameters exist in the control laws, sliding surfaces and predefined settling time all of which are tunable. Also, a proper adjustment of these design parameters used in the proposed control method is done to decrease energy consumption, reduce convergence time and improve tracking performance.

The rest of this paper is arranged as follows. The second section presents the notation, lemmas and mathematical preliminaries used throughout the paper. In the third section, the problem statement is given which includes the nonlinear mathematical model of a 3-DOF ROV and control goal description. The fourth section is devoted to designing the proposed controller using the CFRPSMC method. RPSMC, FSMC and TSMC methods are given in this section. In the fifth section, the comparative simulation results are reported.

An analytical comparison is made among results. The conclusion of this article is given in the last section.

2 Mathematical Preliminaries

2.1 Notation

The following notation is used throughout the paper:

- $\mathbb{R}$ is the set of real numbers; $\mathbb{R}_+ = \{y \in \mathbb{R} | y > 0\}$ and $\mathbb{R}_{\geq 0} = \{y \in \mathbb{R} | y \geq 0\}$.
- For $y \in \mathbb{R}$, y^T signifies its transpose, $|y|$ denotes absolute function, $y = \sqrt{y^T y}$ denotes Euclidean norm and $\exp(y)$ denotes exponential function.
- $\dot{\vartheta}(t) = \frac{\mathrm{d}\vartheta}{\mathrm{d}t}$ and $\ddot{\vartheta}(t) = \frac{\mathrm{d}^2\vartheta}{\mathrm{d}t^2}$ signify the first and the second derivative, respectively, for the function of $\vartheta : \mathbb{R} \to \mathbb{R}$. That is, the dot $(\cdot)$ denotes the differential with respect to time.
- sign(.) signifies the signum function.

2.2 Fundamental Facts

Some standard definitions and lemmas are provided here that are used throughout the paper.

Consider a system (1) as follows

$$\dot{x} = f(t, x; a) \tag{1}$$

where $x \in \mathbb{R}^n$ is the system state and $f : \mathbb{R} \to \mathbb{R}^n$ is a nonlinear function. Also, $a \in \mathbb{R}^b$ with $\dot{a} = 0$ represents the system parameters. The time t is considered on the interval $[t_0, \infty)$, where $t_0 \in \mathbb{R}_+ \cup \{0\}$. The system initial conditions are $x(\mathrm{t}_0) = x_0$.

Definition 1 (*Global finite-time stability* (Bhat and Bernstein 2000; Jiménez-Rodríguez et al. 2017c)). If the origin of system (1) has global asymptotic stability and any solution $x(t, x_0)$ of system (1) converges to the equilibrium point in a finite time for all x_0, i.e., $t \geq T(x_0) : x(t, x_0) = 0$, where $T : \mathbb{R}^n \to$, is said settling time function, then the origin of system (1) has global finite-time stability.

Definition 2 (*Fixed-time stability* (Polyakov 2011; Jiménez-Rodríguez et al. 2017c)). If the origin of system (1) has finite-time stability and the settling time function is bounded, i.e., $\exists T_{\max} \geq 0 : T(x_0) \leq T_{\max}$, for all x_0, then the origin is fixed-time stable.

Definition 3 (*Predefined-time stability* (Sánchez-Torres et al. 2014; Sánchez-Torres et al. 2018b)). For the case of fixed-time stability when the parameters a of system (1) can be chosen such that the settling time function $T_{\max}$ can be predefined as desired, it is said the origin of system (1) has predefined-time stability.

Definition 4 (*Strongly predefined-time stable* (Jiménez-Rodríguez et al. 2017c; Sánchez-Torres et al. 2018b)). For the system parameters a, a nonempty set $M \subset \mathbb{R}^n$ is called globally strongly predefined-time attractive if any solution $x(t, x_0)$ of system (1) converges to M at a finite time $t = t_0 + T(x_0)$, where the settling time function is $\sup T(x_0) = T_c \in \mathbb{R}^n$ and T_c is said the strong predefined time.

Definition 5 (*Weakly predefined-time stable* (Jiménez-Rodríguez et al. 2017c; Sánchez-Torres et al. 2018b)). For the system parameters a, a nonempty set $M \subset \mathbb{R}^n$ is called globally weakly predefined-time attractive for system (1), if any solution $x(t, x_0)$ of system (1) converges to M at a finite time $t = t_0 + T(x_0)$, where the settling time function is $T(x_0) \leq T_c x_0 \in \mathbb{R}^n$; then, T_c is said the weak predefined time.

Lemma 1 (Lyapunov characterization of weak predefined-time stability (Jiménez-Rodríguez et al. 2017c; Sánchez-Torres et al. 2018b)). *With a Lyapunov function of continuous radially unbounded $V : \mathbb{R}^n \to \mathbb{R}_{\geq 0}$ and real numbers $T_c > 0$ and $0 < q \leq 1$ such that $V(0) = 0$, $V(x) > 0 x \neq 0$ and the derivative of V satisfies $\dot{V} \leq -\frac{1}{qT_c} \exp(V^q) V^{1-q}$, then the origin of system (1) is globally weakly predefined-time stable and the weak predefined stabilization time is $T(x_0) \leq T_c$.*

Definition 6 ((Sánchez-Torres et al. 2015; Jiménez-Rodríguez et al. 2017b)). Consider $h \geq 0$. For $x \in \mathbb{R}^n$, define the function (2) as follows

$$|x|^h = \frac{x}{x^{1-h}} \tag{2}$$

where x is the norm of x. Because $\lim_{x \to 0} |x|^h = 0$, for $h > 0$, then it is defined $|0|^h = 0$. Therefore, this function for $h > 0$ is continuous, and it is discontinuous in $x = 0$ for $h = 0$.

Definition 7 (*Predefined-time stabilizing function* (Sánchez-Torres et al. 2015; Jiménez-Rodríguez et al. 2017b)). For $x \in \mathbb{R}^n$, the predefined-time stabilizing function (3) is as follow

$$\Phi_q(x; T_c) = \frac{1}{T_c q} \exp\left(x^q\right) |x|^{1-q} \tag{3}$$

where $T_c > 0$ and $0 < q \leq 1$ also $\dot{\Phi}_q(x; T_c) = \frac{\mathrm{d}\Phi_q(x; T_c)}{\mathrm{d}t}$ exists for all x and T_c.

Lemma 2 (Predefined-time stable dynamical system (Sánchez-Torres et al. 2015; Jiménez-Rodríguez et al. 2017b)). *For every initial condition x_0, the system (4)*

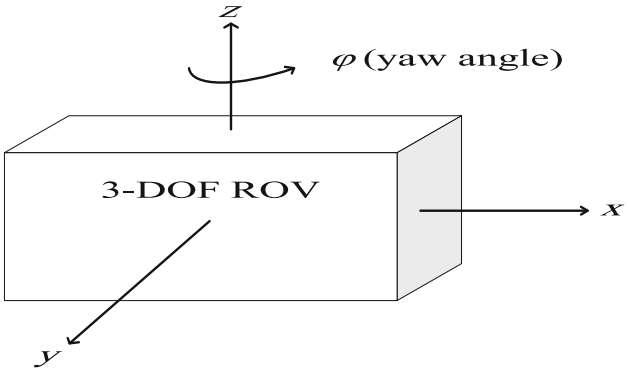

Fig. 2 Configuration of the ROV operation

is globally strongly predefined-time stable with a strong predefined time T_c.

$$\dot{x} = -\Phi_q(x; T_c) \tag{4}$$

where $T_c > 0$ *and* $0 < q \leq 1$. *That is,* $x(t) = 0$ *for all* $t \geq t_0 + T_c$ *in spite of the value of* x_0.

Definition 8 (Wu and Li 2018). The signum function is defined as $\text{sign}(x) = \begin{cases} 1; & x > 0 \\ 0; & x = 0 \\ -1; & x < 0 \end{cases}$ and $|x| = x\text{sign}(x)$ is always true.

Definition 9 (Wu and Li 2018). The $sig(x)$ function is mathematically related to the $\text{sign}(x)$ function as $\text{sig}^a(x) = |x|^a \text{sign}(x)$, where $a \in \mathbb{R}$.

Lemma 3 (Yu et al. 2005) *For positive constants* $a_1, a_2, \ldots, a_n \in \mathbb{R}$ *and* $0 < q < 2$, *inequality* (5) *is always true as follows*

$$\left(a_1^2 + a_2^2 + \ldots + a_n^2\right)^{\frac{q}{2}} \leq |a_1|^q + |a_2|^q + \ldots + |a_n|^q \tag{5}$$

3 Problem Statement

In Fig. 2, a schematic of a 3-DOF (x, y, ϕ) ROV is shown. The ROV is assumed to operate on the surface parallel to the x–y plane to be controlled by the surface vessel. Accordingly, x, y and the yaw angle ϕ are controllable variables of the ROV (Corradini et al. 2010).

3.1 The ROV Nonlinear Model

The mathematical model of a nonlinear 3-DOF ROV has been presented in Corradini et al. (2010), Dyda et al. (2016) and Fossen (2002). This model (6) is given as follows

$$\begin{cases} p_1\ddot{x} + V_x V(p_2|\cos(\phi)| + p_3|\sin(\phi)|) \\ \quad +p_4 x - p_5 V_{cx} V_c = T_x \\ p_1\ddot{y} + V_y V(p_2|\sin(\phi)| + p_3|\cos(\phi)|) \\ \quad \times p_4 y - p_5 V_{cy} V_c = T_y \\ p_6\ddot{\phi} + p_7\dot{\phi}|\dot{\phi}| + p_8 V_c^2 \sin\left(\frac{\phi-\phi_c}{2}\right) + p_9 = M_z \end{cases} \tag{6}$$

where the vector $V = \left[V_x, V_y\right]^T = \left[(\dot{x} - V_{cx}), (\dot{y} - V_{cy})\right]^T$ and the vector $V_c = \left[V_{cx}, V_{cy}\right]^T$ are the vector of velocity in directions x, y, which are considered constants. Also, $p_n, n = (1, 2, \ldots, 9)$ are coefficients that are given in Table 1 (which has been reported in Corradini et al. (2010) based on a case study). Note that the physical characteristics of the vehicle are tied to these coefficients. We have $V_c = \sqrt{V_{cx}^2 + V_{cy}^2}$ and $V = \sqrt{V_x^2 + V_y^2}$. The control inputs are $\left(T_x, T_y, M_z\right) = (u_1, u_2, u_3)$ that should be designed. The angle between the x-axis and the velocity direction of the current is ϕ_c.

3.2 Control Goal

The state variables are defined as $X = [x_1, x_2, x_3, x_4, x_5, x_6]^T = \left[x, \dot{x}, y, \dot{y}, \phi, \dot{\phi}\right]^T$. From a practical point of view, the system should be involved with uncertainties. As a result, the state space nonlinear model of the ROV (7) is obtained as follows

$$\begin{cases} \dot{x}_1 = x_2 \\ \dot{x}_2 = -p_1^{-1}\left(V_x V\begin{pmatrix} p_2|\cos(x_5)| \\ +p_3|\sin(x_5)| \end{pmatrix} + \begin{matrix} \\ +p_4 x_1 - p_5 V_{cx} V_c \end{matrix}\right) + p_1^{-1}u_1 + d_1 \\ \dot{x}_3 = x_4 \\ \dot{x}_4 = -p_1^{-1}\left(V_y V\begin{pmatrix} p_2|\sin(x_5)| \\ +p_3|\cos(x_5)| \end{pmatrix} + \begin{matrix} \\ +p_4 x_3 - p_5 V_{cy} V_c \end{matrix}\right) + p_1^{-1}u_2 + d_2 \\ \dot{x}_5 = x_6 \\ \dot{x}_6 = -p_6^{-1}\left(\begin{matrix} p_7 x_6|x_6| \\ +p_8 V_c^2 \sin\left(\frac{x_5-\phi_c}{2}\right) \\ +p_9 \end{matrix}\right) + p_6^{-1}u_3 + d_3 \end{cases} \tag{7}$$

where $d_j, j = (1, 2, 3)$ are the bounded uncertainties. As the goal of this study is to control the ROV for trajectory tracking, the error model is defined as $e_i = x_i - x_{d_i}, i = (1, 2, \ldots, 6)$, where x_{d_i} are the desired reference tracking trajectories of the system.

Table 1 System parameters with their uncertainties

p_1	12,670 kg ± 10%	p_2	2667 kg m^{-1} ±10%	p_3	4934 kg m^{-1} ±10%
p_4	417 N m^{-1} ±5%	p_5	46,912 kg m^{-1} ±10%	p_6	18,678 kg m^2 ±10%
p_7	9200 kg m^2 ±10%	p_8	−308.4 kg ±5%	p_9	1492 N m ±5%

Assumption 1 (Feng et al. 2014). The uncertainties d_j, $j = (1, 2, 3)$ and its time derivative $\dot{d}_j$, $j = (1, 2, 3)$ are bounded, i.e., the upper bound of uncertainties and its time derivative are given by (8) as follows

$$\begin{cases} |d_j| \le l_j \\ |\dot{d}_j| \le h_j \end{cases} \tag{8}$$

where h_j and l_j are given known constants.

Assumption 2 (Liu et al. 2016). The desired trajectory x_{d_i} and its two-time derivatives are given.

Assumption 3 For $x = [x_1, x_2, \ldots, x_n]^T$, all states of system (6) are measurable.

The tracking error dynamics (9) is obtained as follows

$$\begin{cases} \dot{e}_1 = e_2 \\ \dot{e}_2 = f_1 - \dot{x}_{d_2} + g_1 u_1 + d_1 \\ \dot{e}_3 = e_4 \\ \dot{e}_4 = f_2 - \dot{x}_{d_4} + g_2 u_2 + d_2 \\ \dot{e}_5 = e_6 \\ \dot{e}_6 = f_3 - \dot{x}_{d_6} + g_3 u_3 + d_3 \end{cases} \tag{9}$$

where we have (10) as follows

$$\begin{cases} f_1 = -p_1^{-1}\left(V_x V \begin{pmatrix} p_2|\cos(x_5)| + \\ p_3|\sin(x_5)| \end{pmatrix} + p_4 x_1 \right) \\ \qquad\quad -p_5 V_{cx} V_c \\ f_2 = -p_1^{-1}\left(V_y V \begin{pmatrix} p_2|\sin(x_5)| \\ +p_3|\cos(x_5)| \end{pmatrix} + p_4 x_3 \right), \\ \qquad\quad -p_5 V_{cy} V_c \\ f_3 = -p_6^{-1}\left(p_7 x_6 |x_6| \right. \\ \qquad\quad \left. + p_8 V_c^2 \sin\left(\frac{x_5 - \phi_c}{2}\right) + p_9 \right) \end{cases} \quad \text{and} \quad \begin{cases} g_{1,2} = p_1^{-1} \\ g_3 = p_6^{-1} \end{cases}. \tag{10}$$

The desired tracking trajectories (11) are considered as follows

$$\begin{cases} x_{d_{2j-1}} = \zeta_j(t, x) \\ x_{d_{2j}} = \dot{x}_{d_{2j-1}} = \dot{\zeta}_j(t, x) \end{cases} \quad j = (1, 2, 3). \tag{11}$$

Nonlinear functions $\zeta_j(t, x)$ can be any trajectories for tracking, where $\dot{\zeta}_j(t, x)$ are available.

4 Stability Analysis Using Predefined-Time SMC Scheme

The predefined-time stability analysis based on SMC technique in both the reaching phase and the sliding phase of the closed-loop system is investigated and presented in this section by using Lyapunov stability theory. To establish predefined-time stability analysis utilizing SMC scheme, the following two phases are required:

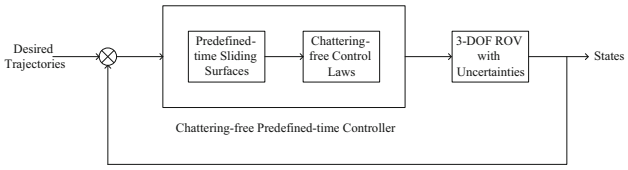

Fig. 3 Block diagram of the proposed method

(1) Reaching phase: ensuring the designed control law can drive the tracking errors onto the defined sliding surface in a predefined time, i.e., the reachability of the tracking errors onto the sliding surface should be achieved in a predefined time.
(2) Sliding phase: ensuring that the sliding mode motion can fulfil the control objective (convergence tracking errors to zero) in a predefined time and maintain it afterwards, i.e., the predefined-time stability of sliding motion ($s = 0$) should be guaranteed.

In the following, a new form of sliding surfaces is proposed. The control inputs (u_1, u_2, u_3) are designed to control the 3-DOF ROV with a predefined-time trajectory tracking goal and to eliminate the chattering phenomenon. A schematic block diagram of the proposed chattering-free predefined-time sliding mode tracking controller for the 3-DOF ROV with uncertainties is illustrated in Fig. 3.

The tracking error dynamics (12) is considered as follows

$$\begin{cases} \dot{e}_{2j-1} = e_{2j} \\ \dot{e}_{2j} = f_j + g_j u_j - \dot{x}_{d_{2j}} + d_j; \end{cases} \quad j = (1, 2, 3). \tag{12}$$

The sliding surfaces (13) are defined as follows

$$\begin{cases} s_{2j-1} = \dot{e}_{2j-1} + \Phi_{q_{2j-1}}\left(e_{2j-1}; T_{c_{2j-1}}\right) \\ s_{2j} = \dot{s}_{2j-1} + \Phi_{q_j}\left(s_{2j-1}; T_{c_{2j}}\right) \end{cases} \tag{13}$$

where the definition of $\Phi_{q_j}\left(e_{2j-1};T_{c_{2j-1}}\right)$ and $\Phi_{q_j}\left(s_{2j-1};T_{c_{2j}}\right)$ are given by (3). The control laws (14) are defined as follows

$$u_j = g_j^{-1}\begin{pmatrix} -f_j + \dot{x}_{d_{2j}} - \dot{\Phi}_{q_{2j-1}}\left(e_{2j-1};T_{c_{2j-1}}\right) \\ -\Phi_{q_j}\left(s_{2j-1};T_{c_{2j}}\right) \\ -\int \left(h_j + l_j\right)\mathrm{sign}\left(s_{2j}\right)\mathrm{d}t \\ -\int \frac{1}{\left(\sqrt{2}\right)^{\beta_j+1} p_j T_{c_{f_j}}} \exp(V^{p_j})\mathrm{sig}^{\beta_j}\left(s_{2j}\right)\mathrm{d}t \end{pmatrix} \tag{14}$$

where we have $0\Big\langle p_j \le 1, T_{c_{2j}}, T_{c_{2j-1}}, T_{c_{f_j}}\Big\rangle 0$ and $0 < \beta_j \le 1$.

Theorem 1 Let system (12) satisfy Assumptions 1, 2 and 3. The tracking errors reach zero in a predefined time using control laws (14) and sliding surfaces (13), i.e., the ROV states converge to their desired trajectories.

Proof To investigate the predefined-time stability analysis of the above design, the two phases, reaching phase and the sliding phase, require to be obtained as follows:

Phase 1 (reaching phase) The candidate Lyapunov function is defined as $V = \sum_{j=1}^{3} \frac{1}{2} s_{2j}^2$, which satisfies the conditions given in Lemma 1. Taking the time derivative of V yields $\dot{V} = \sum_{j=1}^{3} s_{2j}\dot{s}_{2j}$. Then, taking the time derivative of (13) and substituting in $\dot{V}$, we obtain (15) as follows

$$\begin{aligned} \dot{V} &= \sum_{j=1}^{3}\Bigg(-\frac{1}{\left(\sqrt{2}\right)^{\beta_j+1} p_j T_{c_{f_j}}} \exp\left(V^{p_j}\right)\left|s_{2j}\right|^{\beta_j+1}\left(s_{2j}\right) \\ &\quad -\left(h_j + l_j\right)\left|s_{2j}\right| + s_{2j}\dot{d}_j\Bigg) \\ \dot{V} &\le \sum_{j=1}^{3}\begin{pmatrix} -\frac{1}{\left(\sqrt{2}\right)^{\beta_j+1} p_j T_{c_{f_j}}} \exp(V^{p_j})\left|s_{2j}\right|^{\beta_j+1}\left(s_{2j}\right) \\ -\left(h_j + l_j\right)\left|s_{2j}\right| + \left|s_{2j}\right|\left|\dot{d}_j\right| \end{pmatrix} \end{aligned} \tag{15}$$

where we have $\left|s_{2j}\right|\left|\dot{d}_j\right| \le h_j\left|s_{2j}\right|$ and $-l_j\left|s_{2j}\right| \le 0$. Then, (15) can be rewritten as (16).

$$\dot{V} \le \sum_{j=1}^{3} -\frac{1}{\left(\sqrt{2}\right)^{\beta_j+1} p_j T_{c_{f_j}}} \exp\left(V^{p_j}\right)\left|s_{2j}\right|^{\beta_j+1}\left(s_{2j}\right) \tag{16}$$

According to Lemma 3, we have $\sqrt{2V} \le \sum_{j=1}^{3}\left|s_{2j}\right|^{\beta_j+1}$. Subsequently, (16) can be rewritten as (17).

$$\begin{aligned} &\dot{V} \le -\frac{1}{\left(\sqrt{2}\right)^{\beta_j+1} p_j T_{c_{f_j}}} \exp(V^{p_j})\,(2V)^{\frac{\beta_j+1}{2}} \quad \xRightarrow{\left(\sqrt{2}\right)^{\beta_j+1} T_{c_{f_j}} = T_{p_j}} \\ &\dot{V} \le -\frac{1}{p_j T_{p_j}} \exp(V^{p_j})\,(V)^{\frac{\beta_j+1}{2}} \end{aligned} \tag{17}$$

Considering $\beta_j = 1 - 2p_j$, we obtain (18) as follows.

$$\dot{V} \le -\frac{1}{p_j T_{p_j}} \exp\left(V^{p_j}\right) V^{1-p_j} \tag{18}$$

Based on Lemma 1, we have $s_{2j} \to 0$ in a predefined time presented by (19).

$$T_1 \le \sum_{j=1}^{3} T_{p_j} \tag{19}$$

Therefore, the reaching phase is ensured in a predefined time T_1.

Phase 2 (sliding phase: Using (13) and $s_{2j} = 0$, we have (20) as follows.

$$0 = \dot{s}_{2j-1} + \Phi_{q_j}\left(s_{2j-1};T_{c_{2j}}\right) \to \dot{s}_{2j-1} = -\Phi_{q_j}\left(s_{2j-1};T_{c_{2j}}\right) \tag{20}$$

According to Lemma 2, we obtain $s_{2j-1} = 0$ in a predefined time. Then, we obtain (21) as follows.

$$\begin{aligned} 0 &= \dot{e}_{2j-1} + \Phi_{q_{2j-1}}\left(e_{2j-1};T_{c_{2j-1}}\right) \\ &\to \dot{e}_{2j-1} = -\Phi_{q_{2j-1}}\left(e_{2j-1};T_{c_{2j-1}}\right) \end{aligned} \tag{21}$$

Similarly, based on Lemma 2, we obtain $\mathrm{e}_{2j-1} = 0$. Then, using (12) we obtain $\dot{e}_{2j-1} = e_{2j} = 0$. Hence, the sliding phase is ensured in a predefined time presented by (22).

$$T_2 \le \sum_{j=1}^{3}\left(t_{0j} + T_{c_{2j-1}} + T_{c_{2j}}\right) \tag{22}$$

This concludes the proof. □

Remark 1 Considering phases 1 and 2 in Theorem 1, the predefined-time tracking for the ROV (7) is ensured in a predefined time as $T = T_1 + T_2$, where T_1 and T_2 are given by (19) and (22), respectively.

Remark 2 The parameters β_j, p_j, q_i, $T_{c_{f_j}}$, $T_{c_{2j}}$ and $T_{c_{2j-1}}$ in the sliding surfaces (13), the control laws (14) and the predefined stabilization time T are tunable design parameters. Thus, the control efforts and the system convergence time can be adjusted by selecting them properly.

The configuration of the presented design algorithm is displayed in Fig. 4.

Proposition 1 *Let system* (12) *satisfy Assumptions* 1, 2*and* 3. *The tracking errors reach zero in a predefined time, using control laws* (24) *and sliding surfaces* (23). *Note that conventional forms of sliding surfaces and control laws are*

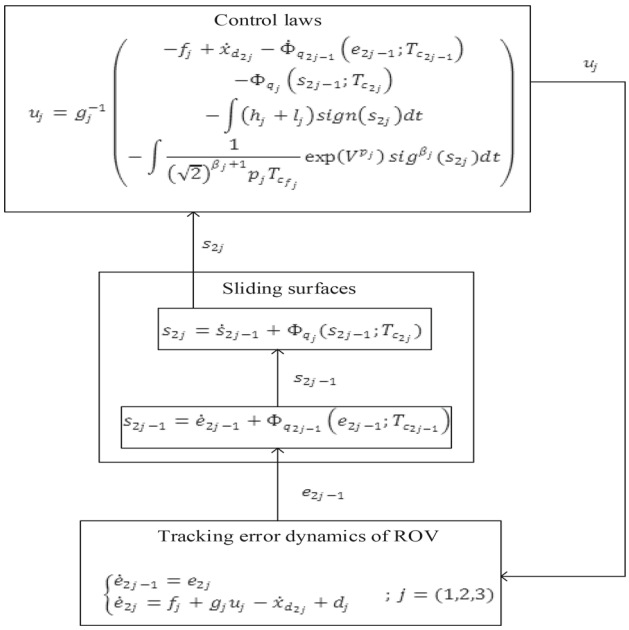

Fig. 4 Flowchart of the proposed design algorithm

considered in this RPSMC method, which is likely to create chattering problem (Remark 3).

$$s_j = \dot{e}_{2j-1} + \Phi_{q_j}(e_{2j-1};T_{c_j}) \tag{23}$$

where the definition of $\Phi_{q_j}(e_{2j-1};T_{c_j})$ *is given by* (3).

$$u_j = g_j^{-1}\begin{pmatrix} -f_j + \dot{x}_{d_{2j}} \\ -\dot{\Phi}_{q_j}(e_{2j-1};T_{c_j}) \\ -l_j sign(s_j) \\ -\frac{1}{(\sqrt{2})^{\beta_j+1} p_j T_{c_{f_j}}} \exp(V^{p_j}) sig^{\beta_j}(s_j) \end{pmatrix} \tag{24}$$

where we have $0 < p_j \le 1, T_{c_j}, T_{c_{f_j}} > 0$ *and* $0 < \beta_j \le 1$. *Also, we have* $|d_j| \le l_j$ *(given by* (8)*).*

The proof of this proposition is similar to that of Theorem 1.

Proposition 2 *Let system* (12) *satisfy Assumptions* 1, 2*and* 3. *The tracking errors reach zero in a fixed time, using control laws* (26) *and sliding surfaces* (25)*, and by utilizing FSMC technique. (The idea behind this scheme is similar to the one given in (Zuo* 2014*).)*

$$\begin{cases} s_{2j-1} = \dot{e}_{2j-1} + A_{2j-1}(e_{2j-1}) + B_{2j-1}(e_{2j-1}) \\ s_{2j} = \dot{s}_{2j-1} + A_{2j}(s_{2j-1}) + B_{2j}(s_{2j-1}) \end{cases} \tag{25}$$

where we have $A_i(\xi) = a_{2i-1}\xi^{\frac{p_{2i-1}}{q_{2i-1}}}$, $B_i(\xi) = a_{2i}\xi^{\frac{p_{2i}}{q_{2i}}}$, $a_j > 0$, $0 < q_{2i-1} < p_{2i-1} < 2q_{2i-1}$ *and* $0 < p_{2i} < q_{2i}$. *Also,* q_{2i-1}, p_{2i-1}, q_{2i} *and* p_{2i} *must be odd numbers to avoid singularity problem.*

$$u_j = g_j^{-1}(t,x)\begin{pmatrix} -f_j(t,x) - \dot{A}_{2j-1}(e_{2j-1}) \\ -\dot{B}_{2j-1}(e_{2j-1}) - A_{2j}(s_{2j-1}) \\ -B_{2j}(s_{2j-1}) \\ -\int r_{2j-1}\mathrm{sig}^{\gamma_{2j-1}}(s_{2j})\mathrm{d}t \\ -\int r_{2j}\mathrm{sig}^{\gamma_{2j}}(s_{2j})\mathrm{d}t \\ -\int (h_j + l_j)\mathrm{sign}(s_{2j})\mathrm{d}t \end{pmatrix} \tag{26}$$

where we have $r_{1,2} > 0$ *and* $1 < \gamma_2, 0 < \gamma_1 < 1$.*Its proof is similar to the proof of Theorem* 1.

Proposition 3 *Let system* (12) *satisfy Assumptions* 1, 2*and* 3. *The tracking errors reach zero in a finite time, using control laws* (28) *and sliding surfaces* (27)*, and by utilizing TSMC technique. (The idea behind this scheme is similar to the one given in (Zuo and Tie* 2016*).)*

$$\begin{cases} s_{2j-1} = \dot{e}_{2j-1} + A_{2j-1}(e_{2j-1}) \\ s_{2j} = \dot{s}_{2j-1} + A_{2j}(s_{2j-1}) \end{cases} \tag{27}$$

where we have $A_i(\xi) = a_{2i-1}\xi^{\frac{p_{2i-1}}{q_{2i-1}}}$, $a_i > 0$, *and* $0 < p_{2i-1} < q_{2i-1}$. *Also,* p_{2i-1} and q_{2i-1} *must be odd numbers to avoid singularity problem.*

$$u_j = g_j^{-1}(t,x)\begin{pmatrix} -f_j(t,x) - \dot{A}_{2j-1}(e_{2j-1}) \\ -A_{2j}(s_{2j-1}) \\ -\int r_{2j-1}\mathrm{sig}^{\gamma_{2j-1}}(s_{2j})\mathrm{d}t \\ -\int (h_j + l_j)\mathrm{sign}(s_{2j})\mathrm{d}t \end{pmatrix} \tag{28}$$

where we have $r_1 > 0$ *and* $0 < \gamma_{2j-1} < 1$. *The proof is analogous to the proof of Theorem* 1.

Remark 3 It is worthwhile to mention that the chattering problem is likely to exist in the control signals of RPSMC and the control scheme given in (Dyda et al. 2016) because of using signum function in their control laws (given by (24) and (35), respectively). However, this unwanted phenomenon is expected to ease in the control signals of the CFRPSMC, FSMC, and TSMC by using the integral of signum function in their control laws (given by (14), (26) and (28), respectively).

Remark 4 The nonlinear dynamical model of the considered 3-DOF ROV (6) is in a form of double integrator systems. A wide group of practical systems can be described with this form of the dynamical model, which includes n independent double integrator subsystems, such as the ship course system (Sun and Chen 2016), two-link robotic manipulators (Liu and Zhang 2014), MEMS system (Ranjbar et al. 2019) and quadrotor (Modirrousta and Khodabandeh 2015). Hence, by adjusting the proposed control scheme design, the predefined control scheme can be applied to control a huge group of practical systems.

5 Simulation and Comparison

In this section, the efficacy of the proposed CFRPSMC scheme is verified by performing simulation for the 3-DOF ROV (6) and providing an analytical comparison with RPSMC, FSMC and TSMC (given in Proposition 1, 2 and 3, respectively) in the first subsection. Then, in the second subsection an analytical comparison is presented between CFRPSMC scheme and a relevant study for the 3-DOF ROV (6) given in (Dyda et al. 2016). The numerical simulation is performed by using Simulink/MATLAB with numerical method ode4 and step size 0.001.

To provide more detailed comparison and assess the performance of the proposed method, the subsequent performance criteria are utilized (given in (Liu and Zhang 2014; Yi and Zhai 2019; Abadi et al. 2018a)).

(i) Integral of the absolute value of the error (IAE) given by (29)

$$\mathrm{IAE}_{e_i} = \int_0^{t_f} |e_i| \mathrm{d}t \tag{29}$$

(ii) Integral of the time multiplied by the absolute value of the error (ITAE) given by (30)

$$\mathrm{ITAE}_{e_i} = \int_0^{t_f} t|e_i| \mathrm{d}t \tag{30}$$

(iii) Integral of the square value (ISV) of the control input given by (31)

$$\mathrm{ISV}_u = \int_0^{t_f} u^2 \mathrm{d}t \tag{31}$$

where t_f is the total running time. The ITAE and IAE give the numerical measures of tracking performance for a whole error curve. The IAE provides an intermediate result, while time is as a term in ITAE, heavily emphasizing the errors that occur late in time. The ISV gives the energy consumption.

5.1 Case One of Comparison

In this subsection, the numerical simulation is performed for the 3-DOF ROV (6) using CFRPSMC, RPSMC, FSMC and TSMC approaches and their simulation results are reported. Then, an analytical comparison is provided among results by utilizing the three performance criteria (29), (30) and (31).

The system initial conditions are chosen as $(x_0, y_0, \varphi_0, \dot{x}_0, \dot{y}_0, \dot{\varphi}_0) = (0.5, 0.2, 0.5, 0, 0, 0)$. The desired tracking trajectories are considered as $(x_d, y_d, \varphi_d) = \left(x_{1_d}, x_{3_d}, x_{5_d}\right) = (\cos(2t), \sin(t), t)$. The model of uncertainties is supposed as $d_j = 0.1\sin(0.1t)$. The upper bounds of uncertainties are considered as $l_j = 0.1$, and the upper bounds of the time derivative of uncertainties are considered as $h_j = 0.01$. The selected design parameters for different methods are given in Tables 2 and 3. The design parameters for both CFRPSMC and RPSMC methods are considered identical. It should be noted that all design parameters (given in Tables 2 and 3) are arbitrary constants, which can be tuned by the designer.

Table 2 Selected design parameters for the CFRPSMC and RPSMC methods

	β_j	p_j	$T_{c_{f_j}}$	q_i	$T_{c_{2j}}, T_{c_{2j-1}}$
CFRPSMC & RPSMC	0.2	0.4	0.5	0.9	0.5

Table 3 Selected design parameters for the FSMC and TSMC methods

	a_{2j-1}	a_{2j}	γ_{2j-1}	γ_{2j}	q_{2j-1}	p_{2j-1}	q_{2j}	p_{2j}	r_j
FSMC	1.4	1.4	0.1	1.1	103	105	103	101	1
TSMC	2.8	–	0.1	–	101	103	–	–	10

Remark 5 It is worth pointing out that the notion of predefined-time stability provides an essential feature for the controller that the upper bound of convergence time can be set by the user during the control design and prior to performing numerical simulation that is independent of initial conditions. Worded in another way, by using a predefined-time notion in the controller, the states are driven to the desired trajectories in the desired convergence time-bound which can be set as design parameters. The desired upper bound of convergence time is calculated for the proposed CFRPSMC scheme prior to performing numerical simulation as follows.

Using (19), (22) and Remark 1, we obtain (32) as follows.

$$T = T_1 + T_2 \leq 3\left(T_{p_j} + T_{c_{2j}} + T_{c_{2j-1}} + t_{0_j}\right) \tag{32}$$

Using $T_{p_j} = \left(\sqrt{2}\right)^{\beta_j+1} T_{c_{f_j}}$ (given by (17)) and $T_{c_{2j}}, T_{c_{2j-1}} = 0.5$ (Table 2), we obtain (33) as follows.

$$T \leq 3(0.75 + 0.5 + 0.5 + 0) \leq 5.25 \tag{33}$$

Therefore, the desired upper bound of convergence time is predefined to be 5.25(s).

Remark 6 It is worthwhile mentioning that the convergence times of FSMC and TSMC schemes are set (by adjusting their design parameters during performing simulation) to be approximately equal to the convergence times of CFRPSMC and RPSMC schemes (which are set prior to performing simulation) for comparing them using the performance criteria given by (29), (30) and (31).

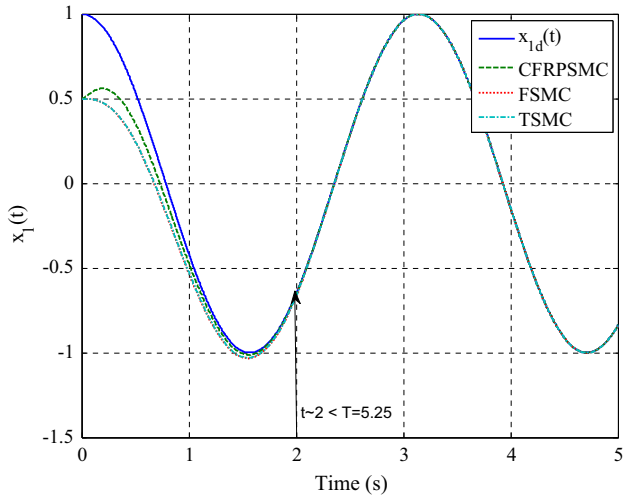

Fig. 5 Time responses of $x_1(t)$ and x_{1_d} of the CFRPSMC, FSMC and TSMC methods

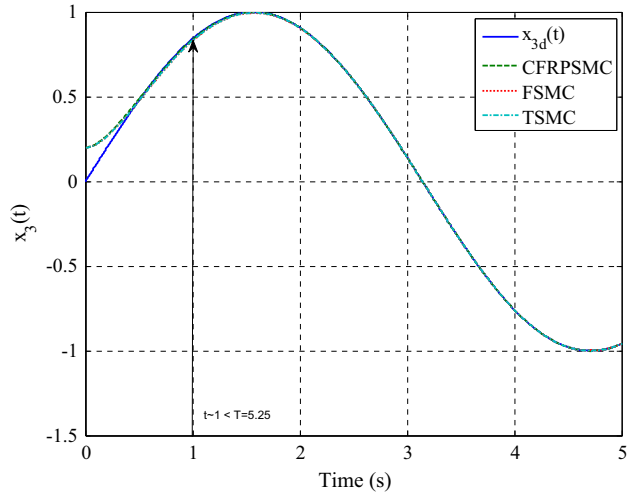

Fig. 7 Time responses of $x_3(t)$ and $x_{3_d}(t)$ of the CFRPSMC, FSMC and TSMC methods

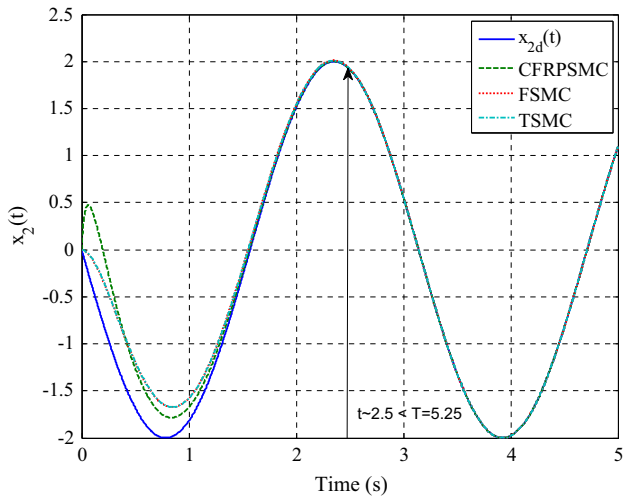

Fig. 6 Time responses of $x_2(t)$ and x_{2_d}(t) of the CFRPSMC, FSMC and TSMC methods

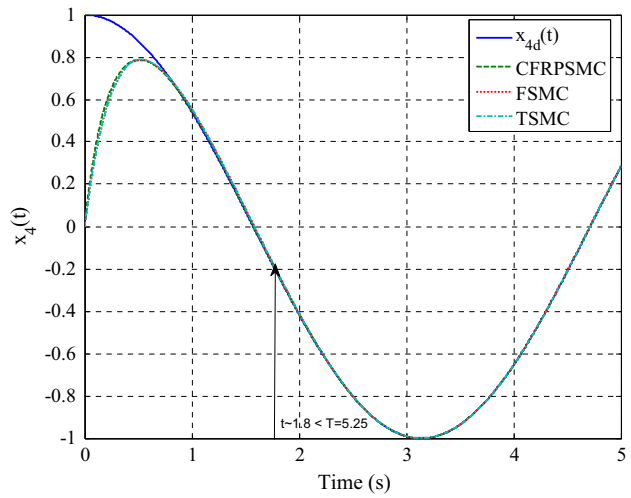

Fig. 8 Time responses of $x_4(t)$ and $x_{4_d}(t)$ of the CFRPSMC, FSMC and TSMC methods

The simulation results of the CFRPSMC, FSMC and TSMC schemes are reported in Figs. 5, 6, 7, 8, 9, 10, 11 and 12. Figure 13 shows the comparative simulation results of the control signal of the CFRPSMC and RPSMC schemes.

The tracking performances of the system states with respect to the desired references are demonstrated in Figs. 5, 6, 7, 8, 9 and 10. It can be seen that the desired references can be reached with suitable tracking performance and high tracking precision after $t \approx 2$(s), $t \approx 2.5$(s), $t \approx 1$(s), $t \approx 1.8$(s), $t \approx 1.5$(s) and $t \approx 2.75$(s) in Figs. 5, 6, 7, 8, 9 and 10, respectively. It should be noticed that the convergence time in Figs. 5, 6, 7, 8, 9 and 10 of CFRPSMC scheme is within $T \leq 5.25$(s), which is determined by (33) in advance as a desired upper bound of predefined convergence time (Remarks 5 and 6). It demonstrates the effectiveness of using a predefined-time notion in the proposed controller.

The tracking errors of $e_1(t)$, $e_2(t)$, $e_3(t)$, $e_4(t)$, $e_5(t)$ and $e_6(t)$ are shown in Fig. 11. Figure 11 shows that the tracking errors reach zero precisely and remain zero afterwards. Figure 12 shows the time responses of the control signals of the CFRPSMC, FSMC and TSMC methods. Figure 12 shows that the chattering problem does not exist in the control signals of the proposed CFRPSMC scheme and the other two schemes: FSMC and TSMC (Remark 3).

The control signals of CFRPSMC and RPSMC are illustrated in Fig. 13. It can be seen that the designed controller of CFRPSMC is continuous without the undesirable chattering phenomenon (Figs. 12 and 13), while the chattering is

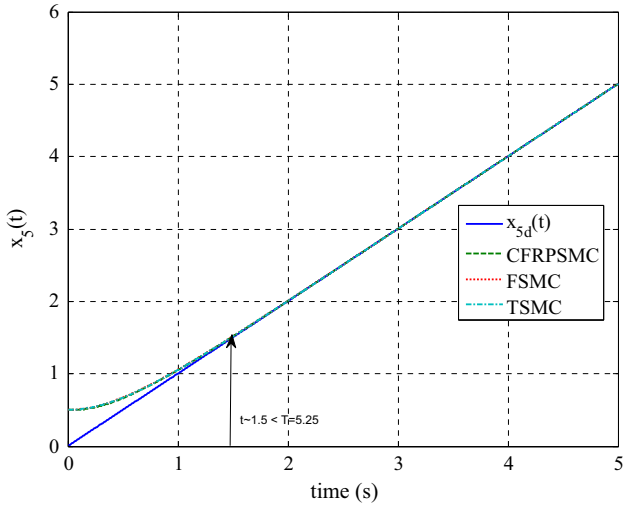

Fig. 9 Time responses of $x_5(t)$ and $x_{5_d}(t)$ of the CFRPSMC, FSMC and TSMC methods

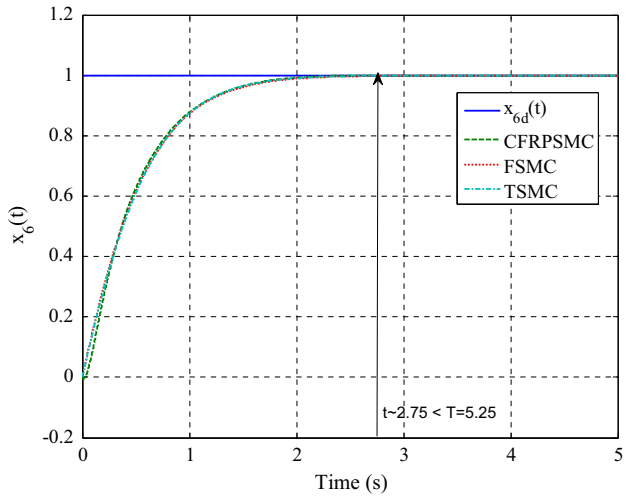

Fig. 10 Time responses of $x_6(t)$ and $x_{6_d}(t)$ of the CFRPSMC, FSMC and TSMC methods

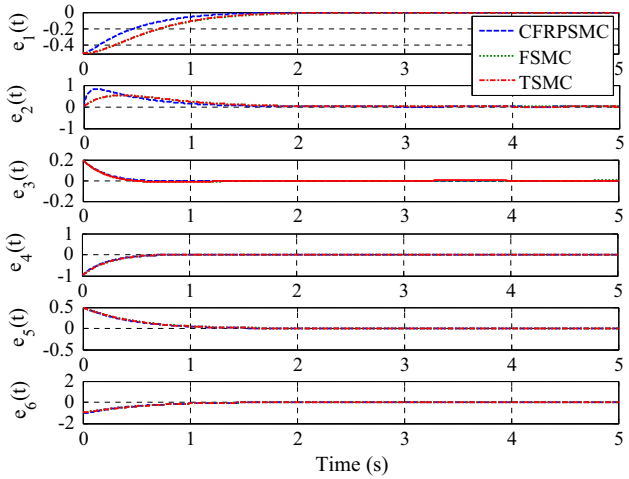

Fig. 11 Time responses of $e_1(t)$, $e_2(t)$, $e_3(t)$, $e_4(t)$, $e_5(t)$ and $e_6(t)$ of the CFRPSMC, FSMC and TSMC methods

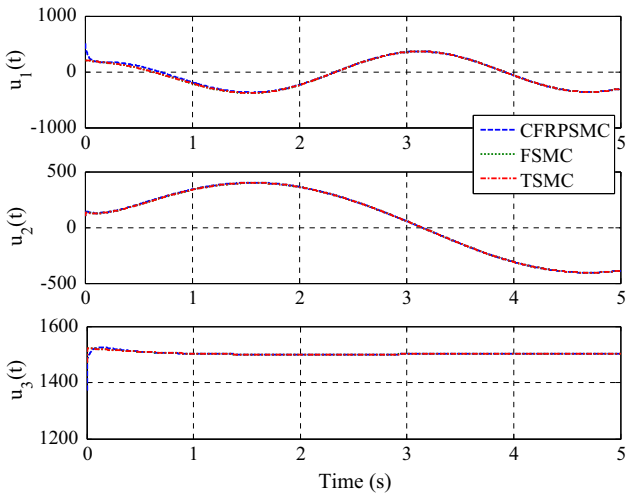

Fig. 12 Time responses of $u_1(t)$, $u_2(t)$ and $u_3(t)$ of the CFRPSMC, FSMC and TSMC methods

observed in the controller of RPSMC (Fig. 13 and Remark 3).

Tables 4, 5 and 6 provide the numerical values of the criteria ISV, IAE and ITAE, respectively, of the CFRPSMC, PSMC, FSMC and TSMC schemes. The comparisons of these performance criteria of the CFRPSMC, PSMC, FSMC and TSMC schemes are shown in Figs. 14, 15 and 16. It is apparent that the proposed CFRPSMC scheme gives lower numerical values (in most cases) for ISV, IAE and ITAE compared with the other three schemes which are RPSMC, FSMC and TSMC. In consequence, the proposed RPSMC scheme outperforms the other three schemes in terms of these three performance criteria given by (29), (30) and (31).

To sum up, the main advantage of CFRPSMC scheme over FSMC and TSMC schemes is that the upper bound of convergence time of CFRPSMC is predefined as desired prior to performing simulation, while the convergence time of FSMC and TSMC is adjusted to be equal to the convergence time of CFRPSMC during performing simulation (Remarks 5 and 6), which takes more consumption of energy for FSMC and TSMC than CFRPSMC (Table 4 and Fig. 14). CFRPSMC provides a better tracking performance compared with the other three methods based on the performance IAE and ITAE (Tables 5, 6 and Figs. 15, 16). The main advantage of CFRPSMC over RPSMC is the elimination of chattering problem.

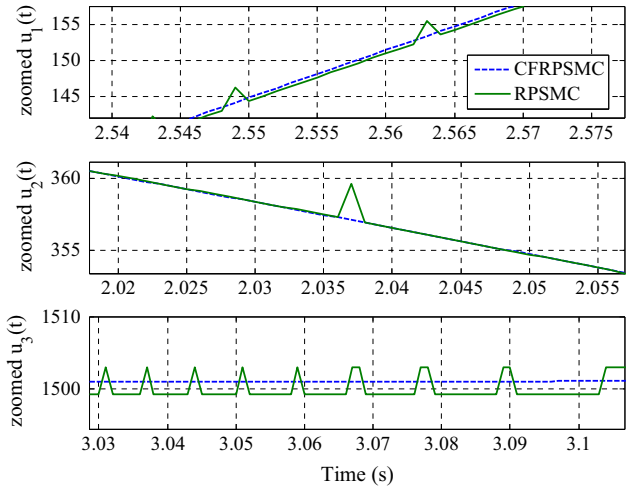

Fig. 13 Time responses of $u_1(t)$, $u_2(t)$ and $u_3(t)$ of the proposed CFRPSMC and the conventional RPSMC

5.2 Case Two of Comparison

In this subsection, the comparative simulation results are provided between the proposed CFRPSMC and a relevant study for the 3-DOF ROV (6) given in (Dyda et al. 2016). Then, an analytical comparison is provided among results. To validate the superiority of the proposed predefined controller in this study, it was compared against the controller given in (Dyda et al. 2016).

The sliding surfaces (34) and control laws (35) of the comparative example are considered as follows (based on (Dyda et al. 2016))

$$\begin{cases} s_{1_x} = \begin{pmatrix} x_{1_d} - x_1 + c_{1x}\left(x_{2_d} - x_2\right)\left|x_{2_d} - x_2\right| \\ +k_{1_x}\left(x_{2_d} - x_2\right) \end{pmatrix} \\ s_{2_x} = \begin{pmatrix} x_{1_d} - x_1 + c_{2x}\left(x_{2_d} - x_2\right)\left|x_{2_d} - x_2\right| \\ +k_{2_x}\left(x_{2_d} - x_2\right) \end{pmatrix} \\ s_{1_y} = \begin{pmatrix} x_{3_d} - x_3 + c_{1y}\left(x_{4_d} - x_4\right)\left|x_{4_d} - x_4\right| \\ +k_{1_y}\left(x_{4_d} - x_4\right) \end{pmatrix} \\ s_{2_y} = \begin{pmatrix} x_{3_d} - x_3 + c_{2y}\left(x_{4_d} - x_4\right)\left|x_{4_d} - x_4\right| \\ +k_{2_y}\left(x_{4_d} - x_4\right) \end{pmatrix} \\ s_{1_\phi} = \begin{pmatrix} x_{5_d} - x_5 + c_{1\phi}\left(x_{6_d} - x_6\right)\left|x_{6_d} - x_6\right| \\ +k_{1_\phi}\left(x_{6_d} - x_6\right) \end{pmatrix} \\ s_{2_\phi} = \begin{pmatrix} x_{5_d} - x_5 + c_{2\phi}\left(x_{6_d} - x_6\right)\left|x_{6_d} - x_6\right| \\ +k_{2_\phi}\left(x_{6_d} - x_6\right) \end{pmatrix} \end{cases} \tag{34}$$

and

Table 5 Criterion IAE

	CFRPSMC	RPSMC	FSMC	TSMC
IAE_{e_1} (m)	1.1138	1.1557	1.5868	1.5613
IAE_{e_2} (m)	2.2572	2.2485	2.1451	2.1520
IAE_{e_3} (m)	0.1823	0.2465	0.2058	0.1988
IAE_{e_4} (m)	1.0053	0.9479	1.0877	1.0779
IAE_{e_5} (rad)	0.9856	0.9927	1.0401	1.0218
IAE_{e_6} (rad)	2.2859	2.3142	2.2725	2.2773

Table 6 Criterion ITAE

	CFRPSMC	RPSMC	FSMC	TSMC
ITAE_{e_1} (m s)	0.1002	0.1022	0.1876	0.1787
ITAE_{e_2} (m s)	0.2429	0.2518	0.3551	0.3481
ITAE_{e_3} (m s)	0.0091	0.0145	0.0198	0.0172
ITAE_{e_4} (m s)	0.0452	0.0524	0.0619	0.0588
ITAE_{e_5} (rad s)	0.0634	0.0851	0.0977	0.0923
ITAE_{e_6} (rad s)	0.1859	0.2141	0.2276	0.2229

$$\begin{cases} u_1 = (p_1)\left(-f_1 + u_{0_x}\left(sign\left(s_{1_x}\right) + sign\left(s_{2_x}\right)\right)\right) \\ u_2 = (p_1)\left(-f_2 + u_{0_y}\left(sign\left(s_{1_y}\right) + sign\left(s_{2_y}\right)\right)\right) \\ u_3 = (p_6)\left(-f_3 + u_{0_\phi}\left(sign\left(s_{1_\phi}\right) + sign\left(s_{2_\phi}\right)\right)\right) \end{cases}. \tag{35}$$

The system initial conditions and the desired tracking trajectories are considered as (36) given in (Dyda et al. 2016).

$$\begin{aligned} (x_0, y_0, \varphi_0, \dot{x}_0, \dot{y}_0, \dot{\varphi}_0) &= (0, 0, 0, 0, 0, 0)\,, \ (x_d, y_d, \varphi_d) \\ &= \left(x_{1_d}, x_{3_d}, x_{5_d}\right) = \left(2, 4, \frac{\pi}{6}\right) \end{aligned} \tag{36}$$

The model of uncertainties is supposed as $d_j = 0.1\sin(t)$. The upper bounds of uncertainties are considered as $l_j = 0.1$, and the upper bounds of the time derivative of uncertainties are considered as $h_j = 0.1$. The selected design parameters for both methods are given in Table 7. It should be noted that all design parameters (given in Table 7) are arbitrary constants, which can be tuned by the designer.

Remark 7 As mentioned in Remark 5, the upper bound of convergence time of the proposed predefined-time method, CFRPSMC, can be predefined as desired prior to performing numerical simulation regardless of initial conditions. The

Table 4 Criterion ISV

	CFRPSMC	RPSMC	FSMC	TSMC
$\mathrm{ISV}_{u_1}(v^2)$	7×10^5	7.0014×10^5	7.0125×10^5	7.0200×10^5
$\mathrm{ISV}_{u_2}(v^2)$	1.0063×10^6	1.0250×10^6	1.0075×10^6	1.0084×10^6
$\mathrm{ISV}_{u_3}(v^2)$	2.8322×10^7	2.8329×10^7	2.8331×10^7	2.8333×10^7

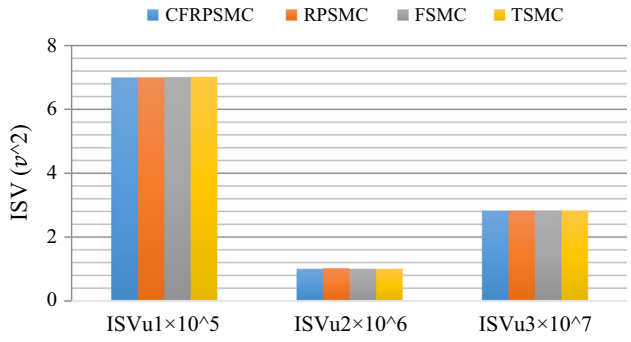

Fig. 14 Comparison of the criterion ISV

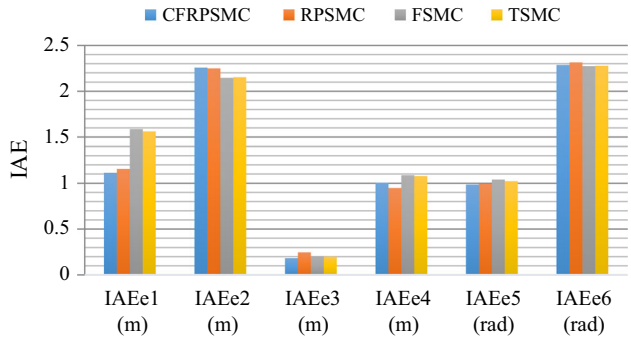

Fig. 15 Comparison of the criterion IAE

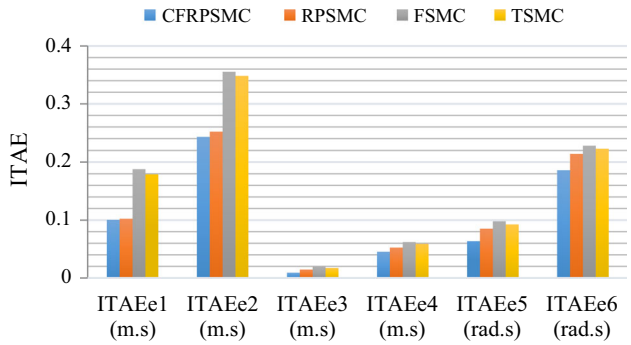

Fig. 16 Comparison of the criterion ITAE

desired upper bound of convergence time is calculated for the CFRPSMC scheme prior to performing numerical simulation as follows.

Using (19), (22) and Remark 1, we obtain (37) as follows.

$$T = T_1 + T_2 \leq 3\left(T_{p_j} + T_{c_{2j}} + T_{c_{2j-1}} + t_{0_j}\right) \tag{37}$$

Using $T_{p_j} = \left(\sqrt{2}\right)^{\beta_j+1} T_{c_{f_j}}$ (given by (17)) and $T_{c_{2j}}, T_{c_{2j-1}} = 10$ (Table 7), we obtain (38) as follows.

$$T \leq 3(4.5 + 10 + 10 + 0) \leq 73.5 \tag{38}$$

Therefore, the desired upper bound of convergence time is predefined to be $73.5(s)$.

Table 7 Selected design parameters

	CFRPSMC		Ref. (Dyda et al. 2016)
β_j	0.2	c_{i_x}	9
p_j	0.1	c_{i_y}	9
$T_{c_{f_j}}$	3	c_{i_ϕ}	9
q_i	0.9	k_{i_x}	10
$T_{c_{2j-1}}$	10	k_{i_y}	10
$T_{c_{2j}}$	10	k_{i_ϕ}	10
–	–	u_{0_x}	15
–	–	u_{0_y}	15
–	–	u_{0_ϕ}	15

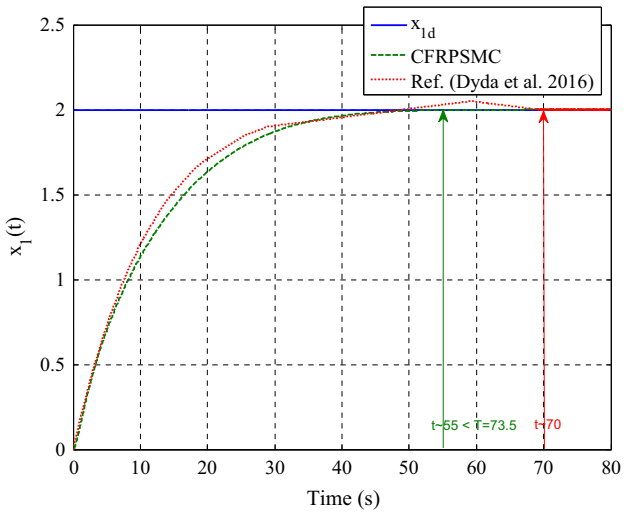

Fig. 17 Time responses of $x_1(t)$ and x_{1_d} of both methods

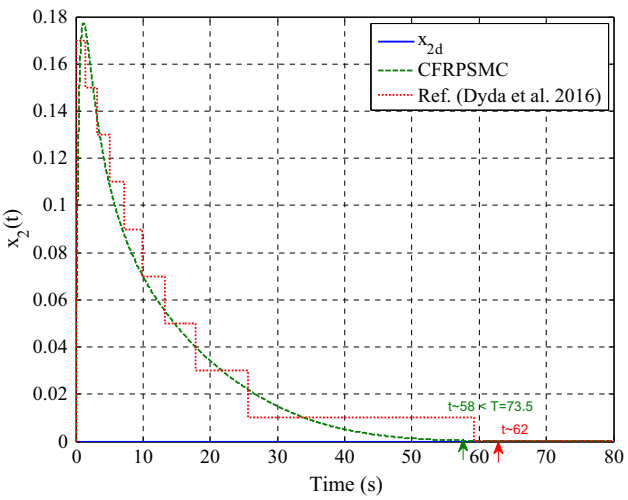

Fig. 18 Time responses of $x_2(t)$ and x_{2_d} of both methods

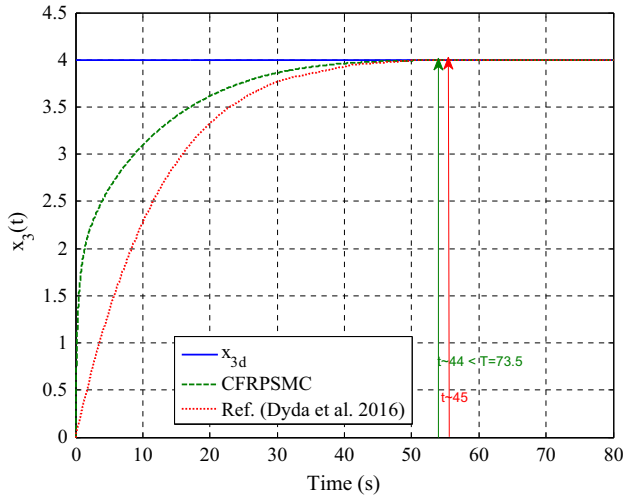

Fig. 19 Time responses of $x_3(t)$ and x_{3_d} of both methods

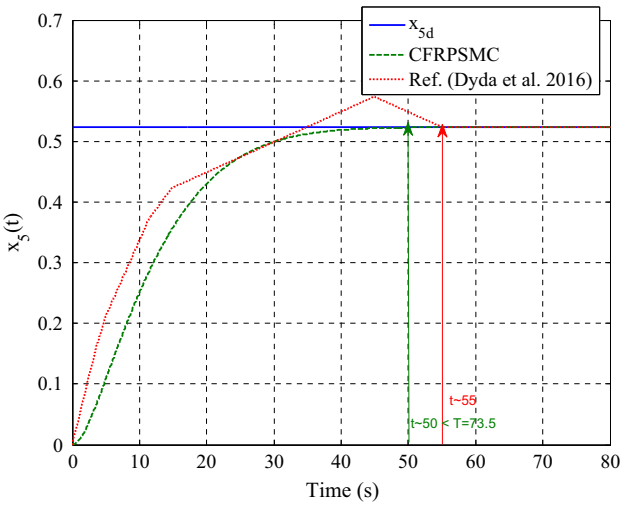

Fig. 21 Time responses of $x_5(t)$ and x_{5_d} of both methods

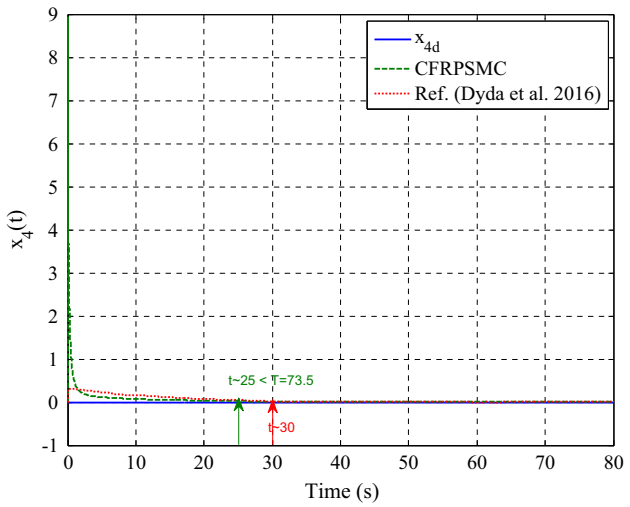

Fig. 20 Time responses of $x_4(t)$ and x_{4_d} of both methods

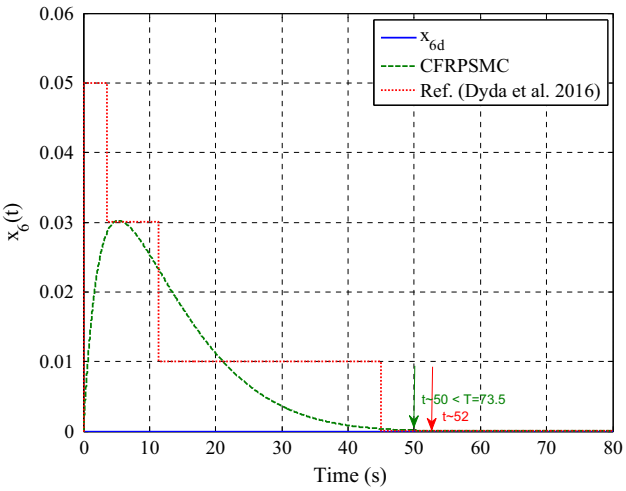

Fig. 22 Time responses of $x_6(t)$ and x_{6_d} of both methods

The comparative simulation results of the proposed controller and the controller given in (Dyda et al. 2016) are reported in Figs. 17, 18, 19, 20, 21, 22, 23, 24, 25 and 26.

The state tracking performances of $x_1(t), x_2(t), x_3(t), x_4(t), x_5(t), x_6(t)$ with respect to the desired references $x_{1_d}(t), x_{2_d}(t), x_{3_d}(t), x_{4_d}(t), x_{5_d}(t), x_{6_d}(t)$ are shown in Figs. 17, 18, 19, 20, 21 and 22, respectively. Figures 17, 18, 19, 20, 21 and 22 show that it takes the proposed controller about $t \approx 55$(s), $t \approx 58$(s), $t \approx 44$(s), $t \approx 25$(s), $t \approx 50$ (s) and $t \approx 50$(s), respectively, to drive the states into the desired states. It takes the controller given in (Dyda et al. 2016) about $t \approx 70$(s), $t \approx 62$(s), $t \approx 45$(s), $t \approx 30$(s), $t \approx 55$(s) and $t \approx 52$(s) in Figs. 17, 18, 19, 20, 21 and 22, respectively, to drive the states into the desired states. Hence, it is obvious that the proposed CFRPSMC provides a faster response than the other method. Figures 17, 18, 19, 20, 21 and 22 show that the proposed CFRPSMC scheme exhibits a better tracking performance than the control scheme given in (Dyda et al. 2016) in terms of convergence rate, tracking precision, smooth tracking, and reducing overshoot and lower shoot. In addition, the efficacy and correctness of the proposed predefined-time method is proved because the convergence time in Figs. 17, 18, 19, 20, 21 and 22 of the CFRPSMC scheme is within $T \leq 73.5$(s), which is predefined by (38) as a desired maximum convergence time (Remark 7).

Figure 23 demonstrates the tracking state errors of the system. As shown in Fig. 23, the tracking errors of the system states $e_1(t), e_2(t), e_3(t), e_4(t), e_5(t)$ and $e_6(t)$ converge to zero accurately by using both methods and remain zero afterwards.

Figures 24, 25 and 26 show time responses of the control signals using both methods. Figures 24, 25 and 26 show

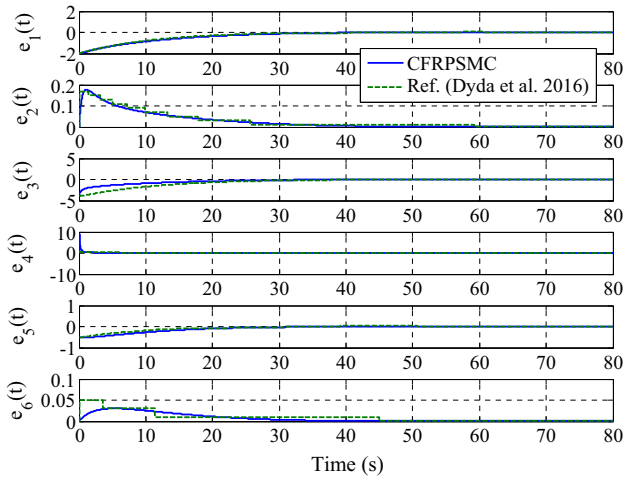

Fig. 23 Time responses of $e_1(t)$, $e_2(t)$, $e_3(t)$, $e_4(t)$, $e_5(t)$ and $e_6(t)$ of both methods

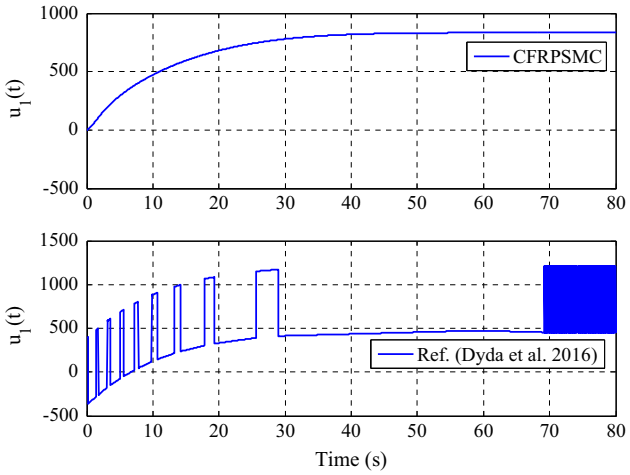

Fig. 24 Time responses of $u_1(t)$ of both methods

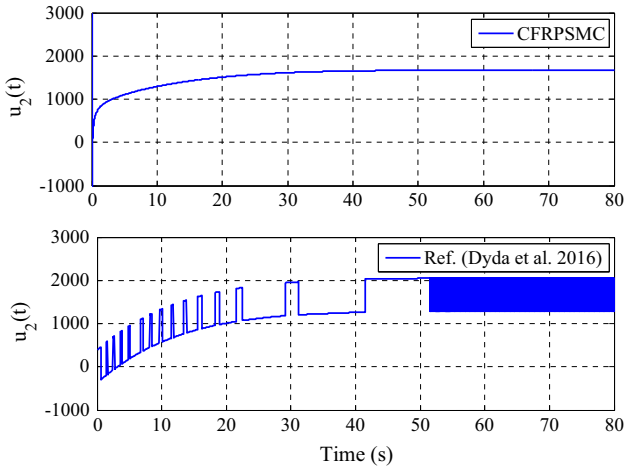

Fig. 25 Time responses of $u_2(t)$ of both methods

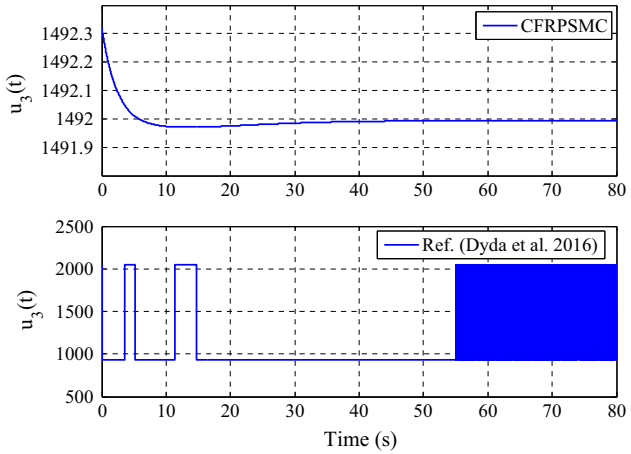

Fig. 26 Time responses of $u_3(t)$ of both methods

Table 8 Criterion ISV

	CFRPSMC	Ref. (Dyda et al. 2016)
$\text{ISV}_{u_1}(v^2)$	2.7342×10^7	4.3927×10^7
$\text{ISV}_{u_2}(v^2)$	1.7670×10^8	2.2294×10^8
$\text{ISV}_{u_3}(v^2)$	1.2769×10^8	1.7808×10^8

Table 9 Criterion IAE

	CFRPSMC	Ref. (Dyda et al. 2016)
IAE_{e_1} (m)	21.3843	22.7043
IAE_{e_2} (m)	2.001	2.2572
IAE_{e_3} (m)	24.5811	44.6251
IAE_{e_4} (m)	3.9986	4.0738
IAE_{e_5} (rad)	5.4919	6.5047
IAE_{e_6} (rad)	0.5234	0.7494

that the control signal of CFRPSMC scheme is continuous without the chattering problem (Remark 3), while undesirable chattering phenomenon is observed (in Figs. 24, 25 and 26) in the control signal of the method given in (Dyda et al. 2016). It is obvious that the amplitude of the control signal of the CFRPSMC scheme is lower than the other one (Figs. 24, 25 and 26).

Tables 8, 9 and 10 represent the numerical values of the criteria ISV, IAE and ITAE, respectively, of the CFRPSMC scheme and the control method given in (Dyda et al. 2016). These performance criteria are compared in Figs. 27, 28 and 29. It can be observed that the proposed CFRPSMC scheme gives lower numerical values for ISV, IAE and ITAE, compared to the method given in (Dyda et al. 2016). As a result, the proposed method is better than the other method in terms of these three performance criteria given by (29), (30) and (31).

Table 10 Criterion ITAE

	CFRPSMC	Ref. (Dyda et al. 2016)
$ITAE_{e_1}$ (m s)	232.8271	233.5671
$ITAE_{e_2}$ (m s)	22.7131	30.8391
$ITAE_{e_3}$ (m s)	246.7145	445.4563
$ITAE_{e_4}$ (m s)	24.5899	45.2400
$ITAE_{e_5}$ (rad s)	60.7014	66.4101
$ITAE_{e_6}$ (rad s)	6.4927	11.5452

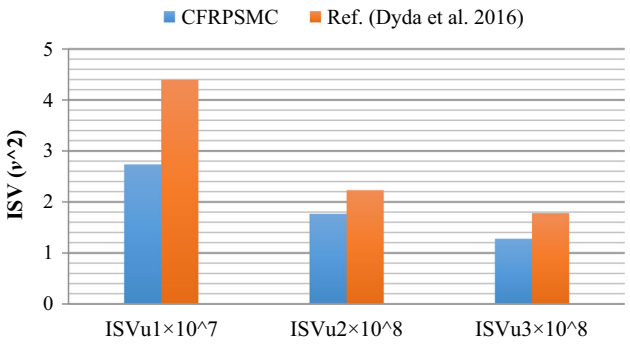

Fig. 27 Comparison of the criterion ISV

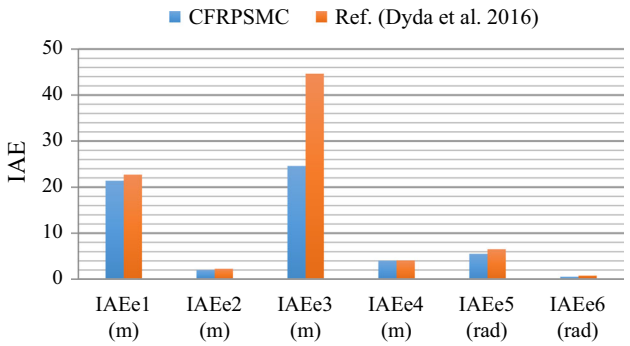

Fig. 28 Comparison of the criterion IAE

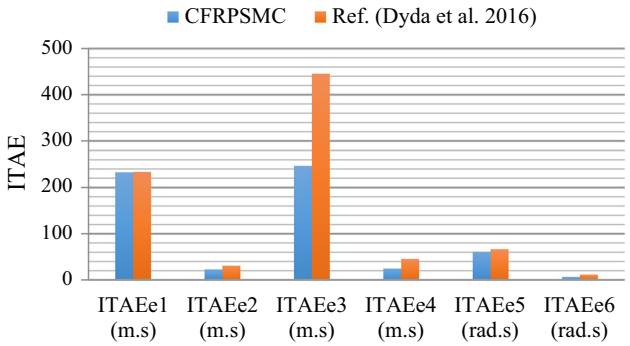

Fig. 29 Comparison of the criterion ITAE

Compared with the results of the control method given in (Dyda et al. 2016), it is concluded that the proposed CFRPSMC method has not only faster convergence property but also less energy consumption, better tracking performance with higher tracking precision, less chattering and predefined convergence time.

6 Conclusion

In this article, the problem of chattering-free robust predefined-time design on the basis of SMC theory has been studied for trajectory tracking of the nonlinear 3-DOF ROV in the presence of matched uncertainties. The proposed CFRPSMC scheme has been designed by incorporating an advanced notion of predefined-time stability, a chattering-free control law, a new form of predefined-time sliding surfaces and a robust sliding mode tracking controller. The advantage of using a predefined-time stability notion in this study is that it provides a desired maximum convergence time regardless of the initial conditions which can be adjusted by the user prior to performing numerical simulation. New forms of sliding surfaces and control laws have been defined such that undesirable chattering phenomenon does not exist in the control signal and both reaching phase and sliding phase have predefined-time convergence property. Corresponding stability analysis of the closed-loop system has been established utilizing Lyapunov stability theory. The analysis of simulation results shows that the desired reference can be attained with superior performance under the designed CFRPSMC approach over the conventional PSMC, FSMC and TSMC control schemes. Also, comparing the proposed scheme with an existing scheme for the 3-DOF ROV in the literature shows the efficacy and superiority of the proposed scheme in this study. In the future, we intend to study state and disturbance observers-based chattering-free fixed-/predefined-time SMC design problem for ROVs with unknown disturbances along with optimizing design parameters.

Acknowledgements The authors would like to thank University of Malaya, Malaysia, for providing financial support under the research grant Impact Oriented Interdisciplinary Research Grant (IIRG): IIRG011A-2019, and Ministry of Higher Education, Malaysia under Large Research Grant Scheme (LRGS): LR008-2019.

Compliance with Ethical Standards

Conflict of interest The authors declare that they have no conflict of interest.

References

Abadi, A. S. S., & Hosseinabadi, P. A. (2017). Nonsingular terminal sliding mode control of ROV system with three methods. In *2017 5th RSI international conference on robotics and mechatronics*

(ICRoM) (pp. 620–623). IEEE. https://doi.org/10.1109/icrom.2017.846623.

Abadi, A. S. S., Hosseinabadi, P. A., & Mekhilef, S. (2018a). Two novel approaches of NTSMC and ANTSMC synchronization for smart grid chaotic systems. *Technology and Economics of Smart Grids and Sustainable Energy, 3*(1), 14. https://doi.org/10.1007/s40866-018-0050-0.

Abadi, A. S. S., Mehrizi, M. H., & Hosseinabadi, P. A. (2018b). Fuzzy adaptive terminal sliding mode control of SIMO nonlinear systems with TS fuzzy model. In *2018 6th Iranian joint congress on fuzzy and intelligent systems (CFIS)* (pp. 185–189). IEEE. https://doi.org/10.1109/cfis.2018.8336620.

Badfar, E., Ardestani, M. A., & Beheshti, M. T. (2020). Robust nonsingular terminal sliding mode control of radius for a bubble between two elastic walls. *Journal of Control, Automation and Electrical Systems*. https://doi.org/10.1007/s40313-019-00558-8.

Becerra, H. M., Vázquez, C. R., Arechavaleta, G., & Delfin, J. (2017). Predefined-time convergence control for high-order integrator systems using time base generators. *IEEE Transactions on Control Systems Technology, 26*(5), 1866–1873. https://doi.org/10.1109/tcst.2017.2734050.

Benosman, M., & Lum, K.-Y. (2009). Passive actuators' fault-tolerant control for affine nonlinear systems. *IEEE Transactions on Control Systems Technology, 18*(1), 152–163. https://doi.org/10.3182/20080706-5-kr-1001.02412.

Berdnikov, V., & Lokhin, V. (2019). Synthesis of guaranteed stability regions of a nonstationary nonlinear system with a fuzzy controller. *Civil Engineering Journal, 5*(1), 107–116. https://doi.org/10.28991/cej-2019-03091229.

Bhat, S. P., & Bernstein, D. S. (2000). Finite-time stability of continuous autonomous systems. *SIAM Journal on Control and Optimization, 38*(3), 751–766. https://doi.org/10.1137/s0363012997321358.

Boonsatit, N., & Pukdeboon, C. (2016). Adaptive fast terminal sliding mode control of magnetic levitation system. *Journal of Control, Automation and Electrical Systems, 27*(4), 359–367. https://doi.org/10.1007/s40313-016-0246-2.

Castillo-García, P., Muñoz Hernandez, L. E., & García Gil, P. (2017). Chapter 7—Sliding mode control**This chapter was developed in collaboration with Efrain Ibarra from the Laboratoire Heudiasyc at the Université de Technologie de Compiegne in France and with M. Jimenez from the Universidad Autonoma de Nuevo Leon in Mexico. In P. Castillo-García, L. E. Muñoz Hernandez, & P. García Gil (Eds.), *Indoor navigation strategies for aerial autonomous systems* (pp. 157–179). Oxford: Butterworth-Heinemann. https://doi.org/10.1016/B978-0-12-805189-4.00010-X.

Chin, C. S., & Lin, W. P. (2018). Robust genetic algorithm and fuzzy inference mechanism embedded in a sliding-mode controller for an uncertain underwater robot. *IEEE/ASME Transactions on Mechatronics, 23*(2), 655–666. https://doi.org/10.1109/tmech.2018.2806389.

Corradini, M. L., Monteriu, A., & Orlando, G. (2010). An actuator failure tolerant control scheme for an underwater remotely operated vehicle. *IEEE Transactions on Control Systems Technology, 19*(5), 1036–1046. https://doi.org/10.1109/tcst.2010.2060199.

Da Cunha, J., Costa, R. R., & Hsu, L. (1995). Design of a high performance variable structure position control of ROVs. *IEEE Journal of Oceanic Engineering, 20*(1), 42–55. https://doi.org/10.1109/48.380247.

Dyda, A., Oskin, D., Longhi, S., & Monteriù, A. (2016). A nonlinear system with coupled switching surfaces for remotely operated vehicle control. *IFAC-PapersOnLine, 49*(23), 311–316. https://doi.org/10.1016/j.ifacol.2016.10.360.

Eaton, R., Katupitiya, J., Pota, H., & Siew, K. W. (2009). Robust sliding mode control of an agricultural tractor under the influence of slip. In *2009 IEEE/ASME international conference on advanced intelligent mechatronics* (pp. 1873–1878). IEEE. https://doi.org/10.1109/aim.2009.5229796.

Elsayed, B. A., Hassan, M. A., & Mekhilef, S. (2015). Fuzzy swinging-up with sliding mode control for third order cart-inverted pendulum system. *International Journal of Control, Automation and Systems, 13*(1), 238–248. https://doi.org/10.1007/s12555-014-0033-4.

Ettefagh, M. H., De Doná, J., Naraghi, M., & Towhidkhah, F. (2017). Control of constrained linear-time varying systems via Kautz parametrization of model predictive control scheme. *Emerging Science Journal, 1*(2), 65–74. https://doi.org/10.28991/esj-2017-01117.

Feng, Y., Han, F., & Yu, X. (2014). Chattering free full-order sliding-mode control. *Automatica, 50*(4), 1310–1314. https://doi.org/10.1016/j.automatica.2014.01.004.

Feng, Y., Yu, X., & Man, Z. (2002). Non-singular terminal sliding mode control of rigid manipulators. *Automatica, 38*(12), 2159–2167. https://doi.org/10.1016/s0005-1098(02)00147-4.

Fernandes, D. D. A., Sorensen, A. J., & Donha, D. C. (2013). Trajectory tracking motion control system for observation class ROVs. *IFAC Proceedings Volumes, 46*(33), 251–256. https://doi.org/10.3182/20130918-4-jp-3022.00025.

Fossen, T. I. (2002). Marine control system-guidance, navigation and control of ships, rigs and underwater vehicles. Marine Cybernetics, Trondheim, Norway. www.marinecybernetics.com

He, S., Song, J., & Liu, F. (2017). Robust finite-time bounded controller design of time-delay conic nonlinear systems using sliding mode control strategy. *IEEE Transactions on Systems, Man, and Cybernetics: Systems, 48*(11), 1863–1873. https://doi.org/10.1109/tsmc.2017.2695483.

Homaeinezhad, M., Yaqubi, S., & Dolatabad, M. A. (2020). Friction-tracker-embedded discrete finite-time sliding mode control algorithm for precise motion control of worm-gear reducers under unknown switched assistive/resistive loading. *Journal of Control, Automation and Electrical Systems*. https://doi.org/10.1007/s40313-020-00583-y.

Hosseinabadi, P. A. (2018). *Finite time control of remotely operated vehicle/Pooyan Alinaghi Hosseinabadi*. Kuala Lumpur: University of Malaya.

Hosseinabadi, P. A., & Abadi, A. S. S. (2019). Adaptive terminal sliding mode control of high-order nonlinear systems. *International Journal of Automation and Control, 13*(6), 668–678. https://doi.org/10.1504/ijaac.2019.102670.

Jiménez-Rodríguez, E., Loukianov, A. G., & Sánchez-Torres, J. D. (2017a). Semi-global predefined-time stable systems. In *2017 14th International conference on electrical engineering, computing science and automatic control (CCE)* (pp. 1–6). IEEE. https://doi.org/10.1109/iceee.2017.8108875.

Jiménez-Rodríguez, E., Sánchez-Torres, J. D., & Loukianov, A. G. (2017b). Predefined-time backstepping control for tracking a class of mechanical systems. *IFAC-PapersOnLine, 50*(1), 1680–1685. https://doi.org/10.1016/j.ifacol.2017.08.492.

Jiménez-Rodríguez, E., Sánchez-Torres, J. D., & Loukianov, A. G. (2017c). On optimal predefined-time stabilization. *International Journal of Robust and Nonlinear Control, 27*(17), 3620–3642. https://doi.org/10.1002/rnc.3757.

Khalid, M. U., Ahsan, M., Kamal, O., & Najeeb, U. (2019). Modeling and trajectory tracking of remotely operated underwater vehicle using higher order sliding mode control. In *2019 16th International Bhurban conference on applied sciences and technology (IBCAST)* (pp. 855–860). IEEE. https://doi.org/10.1109/ibcast.2019.8667200.

Liu, H., & Zhang, T. (2014). Adaptive neural network finite-time control for uncertain robotic manipulators. *Journal of Intelligent and Robotic Systems, 75*(3–4), 363–377. https://doi.org/10.1007/s10846-013-9888-5.

Liu, H., Zhang, T., & Tian, X. (2016). Continuous output-feedback finite-time control for a class of second-order nonlinear systems with disturbances. *International Journal of Robust and Nonlinear Control, 26*(2), 218–234. https://doi.org/10.1002/rnc.3305.

Mobayen, S. (2015). Finite-time tracking control of chained-form non-holonomic systems with external disturbances based on recursive terminal sliding mode method. *Nonlinear Dynamics, 80*(1–2), 669–683. https://doi.org/10.1007/s11071-015-1897-4.

Mobayen, S., Baleanu, D., & Tchier, F. (2017). Second-order fast terminal sliding mode control design based on LMI for a class of non-linear uncertain systems and its application to chaotic systems. *Journal of Vibration and Control, 23*(18), 2912–2925. https://doi.org/10.1177/1077546315623887.

Modirrousta, A., & Khodabandeh, M. (2015). A novel nonlinear hybrid controller design for an uncertain quadrotor with disturbances. *Aerospace Science and Technology, 45,* 294–308. https://doi.org/10.1016/j.ast.2015.05.022.

Munoz-Vazquez, A. J., Torres, J. D. S., Rodriguez, E. J., & Loukianov, A. (2019). Predefined-time robust stabilization of robotic manipulators. *IEEE/ASME Transactions on Mechatronics*. https://doi.org/10.1109/tmech.2019.2906289.

Parsegov, S., Polyakov, A., & Shcherbakov, P. (2012). Nonlinear fixed-time control protocol for uniform allocation of agents on a segment. In *2012 IEEE 51st IEEE conference on decision and control (CDC)* (pp. 7732–7737). IEEE. https://doi.org/10.1109/cdc.2012.6426570.

Parsegov, S., Polyakov, A., & Shcherbakov, P. (2013). Fixed-time consensus algorithm for multi-agent systems with integrator dynamics. 4th IFAC Workshop on Distributed Estimation and Control in Networked Systems, IFAC, Sep 2013, Koblenz, Germany. pp.110–115. https://doi.org/10.3182/20130925-2-de-4044.00055.

Pezeshki, S., Ghiasi, A., Badamchizadeh, M., & Sabahi, K. (2016). Adaptive robust control of autonomous underwater vehicle. *Journal of Control, Automation and Electrical Systems, 27*(3), 250–262. https://doi.org/10.1007/s40313-016-0237-3.

Polyakov, A. (2011). Nonlinear feedback design for fixed-time stabilization of linear control systems. *IEEE Transactions on Automatic Control, 57*(8), 2106–2110. https://doi.org/10.1109/tac.2011.2179869.

Polyakov, A., Efimov, D., & Perruquetti, W. (2015). Finite-time and fixed-time stabilization: Implicit Lyapunov function approach. *Automatica, 51,* 332–340. https://doi.org/10.1016/j.automatica.2014.10.08.

Ranjbar, E., Yaghoubi, M., & Suratgar, A. A. (2019). Adaptive sliding mode controller design for a tunable capacitor susceptible to unknown upper-bounded uncertainties and disturbance. *Iranian Journal of Science and Technology, Transactions of Electrical Engineering*. https://doi.org/10.1007/s40998-019-00220-8.

Sánchez-Torres, J. D., Defoort, M., & Muñoz-Vázquez, A. J. (2018a). A second order sliding mode controller with predefined-time convergence. In *2018 15th International conference on electrical engineering, computing science and automatic control (CCE)* (pp. 1–4). IEEE. https://doi.org/10.1109/iceee.2018.8533952.

Sánchez-Torres, J. D., Gómez-Gutiérrez, D., López, E., & Loukianov, A. G. (2018b). A class of predefined-time stable dynamical systems. *IMA Journal of Mathematical Control and Information, 35*(Supplement_1), i1–i29. https://doi.org/10.1093/imamci/dnx004.

Sánchez-Torres, J. D., Sanchez, E. N., & Loukianov, A. G. (2014). A discontinuous recurrent neural network with predefined time convergence for solution of linear programming. In *2014 IEEE symposium on swarm intelligence* (pp. 1–5). IEEE. https://doi.org/10.1109/sis.2014.7011799.

Sánchez-Torres, J. D., Sanchez, E. N., & Loukianov, A. G. (2015). Predefined-time stability of dynamical systems with sliding modes. In *2015 American control conference (ACC)* (pp. 5842–5846). IEEE. https://doi.org/10.1109/acc.2015.7172255.

Shafiei, M., & Binazadeh, T. (2013). Application of partial sliding mode in guidance problem. *ISA Transactions, 52*(2), 192–197. https://doi.org/10.1016/j.isatra.2012.11.005.

Song, J., Niu, Y., & Zou, Y. (2018). A parameter-dependent sliding mode approach for finite-time bounded control of uncertain stochastic systems with randomly varying actuator faults and its application to a parallel active suspension system. *IEEE Transactions on Industrial Electronics, 65*(10), 8124–8132. https://doi.org/10.1109/tie.2018.2801801.

Sun, X., & Chen, W. (2016). Global generalised exponential/finite-time control for course-keeping of ships. *International Journal of Control, 89*(6), 1169–1179. https://doi.org/10.1080/00207179.2015.1125020.

Taheri, B., Sedaghat, M., Bagherpour, M. A., & Farhadi, P. (2019). A new controller for DC–DC converters based on sliding mode control techniques. *Journal of Control, Automation and Electrical Systems, 30*(1), 63–74. https://doi.org/10.1007/s40313-018-00427-w.

Tchinda, S. T., Mpame, G., Takougang, A. N., & Tamba, V. K. (2019). Dynamic analysis of a snap oscillator based on a unique diode nonlinearity effect, offset boosting control and sliding mode control design for global chaos synchronization. *Journal of Control, Automation and Electrical Systems, 30*(6), 970–984. https://doi.org/10.1007/s40313-019-00518-2.

Tiwari, P. M., Janardhanan, S., & un Nabi, M. (2015). Rigid spacecraft attitude control using adaptive non-singular fast terminal sliding mode. *Journal of Control, Automation and Electrical Systems, 26*(2), 115–124. https://doi.org/10.1007/s40313-014-0164-0.

Van Nguyen, T., Thai, N. H., Pham, H. T., Phan, T. A., Nguyen, L., Le, H. X., et al. (2019). Adaptive neural network-based backstepping sliding mode control approach for dual-arm robots. *Journal of Control, Automation and Electrical Systems, 30*(4), 512–521. https://doi.org/10.1007/s40313-019-00472-z.

Wang, Y., Chen, J., & Gu, L. (2014). Output feedback fractional-order nonsingular terminal sliding mode control of underwater remotely operated vehicles. *The Scientific World Journal*. https://doi.org/10.1155/2014/838019.

Wang, Y., Gu, L., Gao, M., & Zhu, K. (2016a). Multivariable output feedback adaptive terminal sliding mode control for underwater vehicles. *Asian Journal of Control, 18*(1), 247–265. https://doi.org/10.1002/asjc.1013.

Wang, Y., Gu, L., Luo, G., Li, X., Zhou, F., Cao, X., et al. (2015). Depth control of ROVs using time delay estimation with nonsingular terminal sliding mode. In *OCEANS 2015-MTS/IEEE Washington* (pp. 1–6). IEEE. https://doi.org/10.23919/oceans.2015.7401804.

Wang, J., Song, Y., Zhang, S., & Liu, Y. (2016). Modelling, parameters identification and sliding mode control for the pitch control system of an remotely operated vehicle. In *Control conference (CCC), 2016 35th Chinese* (pp. 2146–2150). IEEE. https://doi.org/10.1109/chicc.2016.7553685.

Wang, Y., Yan, F., Tian, B., Gu, L., & Chen, B. (2018). Nonsingular terminal sliding mode control of underwater remotely operated vehicles. *Transactions of the Canadian Society for Mechanical Engineering, 42*(2), 105–115. https://doi.org/10.1155/2014/838019.

Wei, Y., Zhou, W., Chen, W., & Han, H. (2015). Adaptive integral backstepping controller design for ROV with disturbance observer. In *2015 IEEE international conference on mechatronics and automation (ICMA)*, (pp. 1106–1110). IEEE. https://doi.org/10.1109/icma.2015.7237640.

Wu, J., & Li, X. (2018). Finite-time and fixed-time synchronization of Kuramoto-oscillator network with multiplex control. *IEEE Trans-*

actions on Control of Network Systems, 6(2), 863–873. https://doi.org/10.1109/tcns.2018.2880299.

Yang, L., & Yang, J. (2011). Nonsingular fast terminal sliding-mode control for nonlinear dynamical systems. *International Journal of Robust and Nonlinear Control, 21*(16), 1865–1879. https://doi.org/10.1002/rnc.1666.

Yi, S., & Zhai, J. (2019). Adaptive second-order fast nonsingular terminal sliding mode control for robotic manipulators. *ISA Transactions*. https://doi.org/10.1016/j.isatra.2018.12.046.

Yousefi, M., & Binazadeh, T. (2018). Delay-independent sliding mode control of time-delay linear fractional order systems. *Transactions of the Institute of Measurement and Control, 40*(4), 1212–1222. https://doi.org/10.1177/0142331216678059.

Yu, S., Yu, X., Shirinzadeh, B., & Man, Z. (2005). Continuous finite-time control for robotic manipulators with terminal sliding mode. *Automatica, 41*(11), 1957–1964. https://doi.org/10.1016/j.automatica.2005.07.001.

Yu, X., & Zhihong, M. (2002). Fast terminal sliding-mode control design for nonlinear dynamical systems. *IEEE Transactions on Circuits and Systems I: Fundamental Theory and Applications, 49*(2), 261–264. https://doi.org/10.1109/81.983876.

Zaihidee, F. M., Mekhilef, S., & Mubin, M. (2019). Application of fractional order sliding mode control for speed control of permanent magnet synchronous motor. *IEEE Access, 7,* 101765–101774. https://doi.org/10.1109/access.2019.2931324.

Zhou, N., Xia, Y., Wang, M., & Fu, M. (2015). Finite-time attitude control of multiple rigid spacecraft using terminal sliding mode. *International Journal of Robust and Nonlinear Control, 25*(12), 1862–1876. https://doi.org/10.1002/rnc.3182.

Zhu, K., & Gu, L. (2011). A MIMO nonlinear robust controller for work-class ROVs positioning and trajectory tracking control. In *Control and decision conference (CCDC), 2011 Chinese* (pp. 2565–2570). IEEE. https://doi.org/10.1109/ccdc.2011.5968643.

Zuo, Z. (2014). Non-singular fixed-time terminal sliding mode control of non-linear systems. *IET Control Theory and Applications, 9*(4), 545–552. https://doi.org/10.1049/iet-cta.2014.0202.

Zuo, Z., & Tie, L. (2016). Distributed robust finite-time nonlinear consensus protocols for multi-agent systems. *International Journal of Systems Science, 47*(6), 1366–1375. https://doi.org/10.1080/00207721.2014.925608.